Rapid selection of HIV envelopes that bind to neutralizing antibody B cell lineage members with functional improbable mutations

Olivia Swanson[1], Brianna Rhodes[1], Avivah Wang[1], Shi-Mao Xia[1], Cooper Melissa[1], Robert Parks[1], Aja Sanzone[1], Mark K. Louder[5], Bob C. Lin[5], Nicole A. Doria-Rose[5], Kevin O. Saunders[1,3], Mattia Bonsignori[1,2], Kevin Wiehe[1,2], Barton F. Haynes[1,2,4], Mihai L. Azoitei[1,2*]

[1]Duke Human Vaccine Institute, Duke University, Durham, NC

[2]Department of Medicine, Duke University, Durham, NC

[3]Department of Surgery, Duke University, Durham, NC

[4]Department of Immunology, Duke University, Durham, NC

[5] Vaccine Research Center, National Institute of Allergy and Infectious Diseases, National Institutes of Health, Bethesda, MD

* Correspondence: mihai.azoitei@duke.edu

Summary

Elicitation of broadly neutralizing antibodies (bnAbs) by an HIV vaccine will involve priming the immune system to activate antibody precursors, followed by boosting immunizations to select for antibodies with functional features required for neutralization breadth. The higher the number of acquired mutations necessary for function, the more convoluted are the antibody developmental pathways. HIV bnAbs acquire a large number of somatic mutations, but not all mutations are functionally important. Here we identified a minimal subset of mutations sufficient for the function of the naturally occurring V3-glycan bnAb DH270.6. Using antibody library screening, candidate envelope immunogens that interacted with DH270.6-like antibodies containing this set of key mutations were identified and selected *in vitro*. Our results demonstrate that less complex B cell evolutionary pathways than those naturally observed exist for the induction of HIV bnAbs by vaccination, and establish rational approaches to identify boosting sequential envelope candidate immunogens.

Introduction

A major goal of HIV vaccine development is to elicit broadly neutralizing antibodies (bnAbs) (Haynes et al., 2019; Kwong and Mascola, 2018). High levels of bnAbs are rarely observed upon HIV infection (Doria-Rose et al., 2010; Gray et al., 2009) although ~50% of HIV-infected individuals make detectable levels of bnAbs over time (Hraber et al., 2014). When they do occur, bnAbs typically take years to develop and their maturation follows intricate evolutionary pathways that depend on a complex interplay between viral evolution and immune adaptation (Bonsignori et al., 2017b; Bonsignori et al., 2018; Bonsignori et al., 2016; Doria-Rose and Landais, 2019; Gao et al., 2014; Haynes et al., 2016; Liao et al., 2013b; Wu et al., 2015). One strategy of HIV vaccine development mimics the process of natural bnAb formation by targeting the unmutated common ancestor B cell receptors (BCRs) of naïve B cell precursors of bnAb B cells, and using sequential immunogens to guide otherwise disfavored B cell lineage maturation pathways to rapidly acquire the mutations required for broad neutralization (Haynes et al., 2019; Haynes et al., 2012; Kwong and Mascola, 2018).

Compared to neutralizing antibodies against other viruses such as influenza or SARS-CoV-2, HIV bnAbs acquire an unusually large number of somatic mutations, ranging from 11% to 42%, during their evolution from the unmutated common ancestor (UCA) to their mature form (Landais and Moore, 2018; Sok et al., 2013; Wiehe et al., 2018). However, it was previously shown that for two HIV bnAbs, VRC01 and BG18, only about a third of the sequence changes observed in their development of are sufficient to provide neutralization breadth and potency (Jardine et al., 2016; Steichen et al., 2019). Thus it is likely that for other HIV bnAbs only a subset of the acquired mutations are functionally important or needed for vaccine-induced bnAb development (Georgiev et al., 2014; Wiehe et al., 2018).

Recently, it was shown that HIV bnAbs are enriched for improbable mutations acquired during affinity maturation (Shen et al., 2020; Wiehe et al., 2018). These amino acid changes are

48 expected to occur with low frequency naturally, either because they occur in gene regions that
49 are not typically targeted by the Activation-Induced Cytidine Deaminase (AID) or due to the
50 number of nucleotide changes required to transform a respective UCA amino acid into the
51 mature one (Hwang et al., 2017; Yaari et al., 2013). Notably, improbable mutations typically play
52 a critical role in HIV bnAb function and represent developmental barriers that need to be
53 overcome for the development of neutralization breadth (Bonsignori et al., 2017a; Shen et al.,
54 2020). For example, in the evolution of the DH270.6 bnAb, the acquisition of an improbable
55 glycine to arginine mutation at position 57 in the heavy chain initiates the development of
56 heterologous neutralization breadth (Bonsignori et al., 2017a). Similarly, in the VRC34 lineage
57 the only branch that gave rise to bnAbs acquired a rare tyrosine to proline mutation that is
58 essential for broad neutralizing activity (Shen et al., 2020). Since improbable functional
59 mutations represent rare events that restrict bnAb development, antibodies with such sequence
60 changes will likely need to be explicitly selected by candidate immunogens in vaccinations.

61 Significant progress has been made in the design of immunogens that activate
62 precursors of HIV bnAbs such as VRC01, BG18, CH235 and DH270 (Havenar-Daughton et al.,
63 2018; LaBranche et al., 2019; Saunders et al., 2019; Steichen et al., 2016; Steichen et al.,
64 2019). Targeting immunogens against these antibodies have been shown to stimulate B cells
65 displaying the respective UCAs in knock-in mouse models and to promote the early
66 development of bnAb lineages (Dosenovic et al., 2015b; LaBranche et al., 2019; Saunders et
67 al., 2019; Steichen et al., 2019). However, how to further induce maturation of bnAb precursors
68 to attain significant neutralization breadth remains a major challenge. A series of boosting
69 immunizations will be required following germline BCR targeting, with immunogens needed to
70 select for bnAb lineage B cells with rare BCR features required for neutralization breadth, such
71 as CDR loop deletions or insertions, the ability to accommodate HIV Env glycans, or the

72 presence of functionally important improbable amino acids (Bonsignori et al., 2018; Kepler et al.,
73 2014; Klein et al., 2013; Wiehe et al., 2018).

74 The V3-glycan epitope on HIV Env is targeted by diverse HIV bnAbs, such as DH270,
75 PGT121 and BG18 (Barnes et al., 2018; Freund et al., 2017; Julien et al., 2013; Mouquet et al.,
76 2012). Antibodies against this site have different immunogenetics, but all recognize the
77 conserved base of the V3 loop and one or both of the glycans present at positions 301 and 332
78 (Barnes et al., 2018; Mouquet et al., 2012). DH270.6 neutralized 55% of the viruses from a
79 representative global panel of 208 pseudoviruses (IC_{50}=0.08ug/mL) and 77.4% of those viruses
80 containing a glycan at position 332 (Bonsignori et al., 2017a). The induction of DH270.6-like
81 antibodies by vaccination should therefore provide significant protection against HIV infections.
82 Unlike other bnAbs (Walker et al., 2011; Wu et al., 2010), DH270.6 does not acquire any
83 deletions or insertions in its CDR loops during development. Therefore, the elicitation of
84 DH270.6-like bnAbs should be in principle easier to attain, and will require the selection and
85 maturation of putative DH270.6-like precursor antibodies with the key functional somatic
86 mutations present in DH270.6.

87 Recently, a germline targeting immunogen was described that robustly activates
88 DH270.6 precursors in mice (Saunders et al., 2019). This SOSIP Env trimer, named 10.17DT,
89 elicited DH270.6-like antibodies in DH270.6 UCA knock-in mice. Isolated antibodies from
90 animals vaccinated with 10.17DT bound the glycan moiety at position 332 and neutralized both
91 autologous and some heterologous viruses. Importantly, some of the 10.17DT-elicited
92 antibodies acquired improbable mutations from the UCA that are essential for DH270.6 function
93 including heavy chain residues Arg57 and Thr98. The 10.17DT immunogen therefore activates
94 DH270.6 precursors and promotes their acquisition of key functional mutations. In order to
95 mature these responses, additional boosting immunizations will be required to induce high titers
96 of antibodies containing other DH270.6 mutations essential for neutralization breadth and

97 potency. Given the complexity of designing immunogens to guide otherwise disfavored bnAb B
98 cell lineages to neutralization breadth, and the need to speed up immunogen design towards
99 rapid HIV vaccine development, a rapid iterative process is needed to rationally identify
100 sequential immunogens capable of selecting bnAb lineage BCRs containing functional
101 improbable mutations.

102 Here we describe a new approach that relies on computational modeling to identify the
103 functionally important somatic mutations present in HIV bnAbs and a strategy to identify and
104 validate candidate immunogens that select antibodies with these mutations *in vitro*. We illustrate
105 this approach by rapidly identifying the minimal functional mutations in V3-glycan bnAb B cell
106 lineage DH270.6. A subset of 12 out of the 42 acquired mutations accounted for most of the
107 DH270.6 breadth and potency. The resulting minimized DH270.6 (DH270min) antibody that
108 contained these functional mutations represented a bnAb evolutionary path that is shorter and
109 less complex to induce by vaccination. Since the majority of the acquired mutations necessary
110 for the function of DH270.6 were found to be improbable, antibodies containing these amino
111 acids are predicted to occur with low frequency *in vivo.* Consequently, immunogens will have to
112 explicitly target antibody improbable mutation enrichment in order to induce robust protection by
113 vaccination (Wiehe et al., 2018). To address this issue, we developed a new approach for
114 immunogen design that relies on high throughput screening of antibody libraries to identify
115 envelopes that interact with DH270.6-derived antibodies through the key acquired mutation.
116 Alternative recognition modes of DH270min that employ more probable amino acids at some of
117 the key functional sites were explored. This work illustrates a general approach to identify key
118 functional mutations in HIV bnAbs and describes a high throughput method to rationally
119 discover immunogens that target antibody functional mutations.

120 **Results**

121 **Identification of a subset of DH270.6 acquired mutations sufficient for**
122 **neutralization function**. DH270.6 acquired 42 mutations during its development from the UCA
123 to the mature, broadly neutralizing antibody form. Fourteen of these mutations are predicted to
124 be improbable, i.e. they are expected to occur with low frequency prior to antigenic selection in
125 the germinal center, based on computational simulations with ARMADiLLO (Wiehe et al., 2018).
126 Structural mapping revealed that 14 mutations interact directly with the viral envelope, while the
127 other 28 are located far away from the paratope (Figure 1A). This finding suggests that, as
128 previously shown for other HIV bnAbs (Jardine et al., 2016; Steichen et al., 2019), not all of the
129 DH270.6 acquired mutations are required for broad and potent HIV neutralization. While
130 sequence changes located in the paratope are likely important for function, mutations away from
131 the binding interface could also play an important role in the stability and conformation of the
132 antibody. We used computational modeling with Rosetta (Bender et al., 2016; Das and Baker,
133 2008; Leaver-Fay et al., 2011) to identify acquired mutations away from the paratope that could
134 affect function. On the backbone of the DH270.6 scFv (PDBID: 6cbp), acquired mutations
135 deemed nonessential were reversed to their UCA identity and the energetics of the new
136 antibodies were assessed computationally (Supplementary Figure 1A). Upon analysis of
137 different sets of acquired mutations, two “minimized” antibodies, DH270min1 and DH270min2,
138 that contained only 17 and 20 of the 42 mutations acquired by DH270.6 respectively, were
139 determined to have energies comparable to DH270.6 by Rosetta (Supplementary Figure 1B),
140 and were subsequently selected for experimental characterization. Both DH270min1 and
141 DH270min2 included acquired mutations located at the binding interface as well as improbable
142 mutations located immediately adjacent to the paratope (Figure 1A, B). DH270min2 contained
143 additional mutations at the interface of the heavy and light chains. Three other antibodies were
144 also tested as reference: DH270min3, that contained only the DH270.6 acquired mutation
145 located in the paratope, as well as DH270Improb and DH270Prob that contained only the
146 acquired improbable and probable mutations, respectively. The Rosetta energy of DH270min3

147 (Supplementary Figure 1B) was less favorable than that of DH270.6, DH270min1 or
148 DH270min2, suggesting that acquired mutations located outside the paratope play an important
149 structural role. Antibodies were expressed recombinantly, purified as IgGs, and tested for
150 neutralization on a representative panel of 15 DH270.6-sensitive HIV pseudoviruses (Figure
151 1C). Both DH270min1 and DH270min2 had the same neutralization breadth and potency on this
152 panel as WT DH270.6, revealing that less than half of the acquired mutations are sufficient for
153 DH270.6 function. In contrast, DH270min3 showed significantly reduced breadth (66%) and
154 potency (0.99μg/mL compared to 0.09μg/mL in DH270.6), confirming the Rosetta modeling
155 prediction that antibody residues outside the binding interface are functionally important.
156 Remarkably, even though there are twice as many probable mutations as improbable in
157 DH270.6, DH270Improb retained 80% of the DH270.6 breadth, while DH270Prob did not
158 neutralize any of the viruses in the panel. Both DH270min1 and DH270min2 contain 13 of the
159 total 14 improbable mutations acquired by DH270.6, showing that improbable mutations are
160 essential for the function of this bnAb.

161 We next determined whether all of the 17 acquired mutations present in DH270min1
162 were necessary for its breadth, or if the antibody can be further "minimized" by reverting
163 additional amino acids to their UCA identity. Single mutant DH270min1 antibody variants, where
164 each of the acquired amino acids maintained from DH270.6 were changed to the corresponding
165 UCA residue, were expressed recombinantly and tested for neutralization as before (Figure 2A).
166 Changing five of the acquired amino acids ($F32Y_{HC}$, $Q54N_{HC}$, $T60Y_{HC}$, $K26S_{LC}$, $H32Y_{LC}$) to their
167 DH270UCA identity had no effect on the breadth or potency of the resulting DH270min1
168 variants; five mutations to UCA ($D31G_{HC}$, $M51I_{HC}$, $T55S_{HC}$, $G94S_{LC}$, $A97S_{LC}$) had a moderate
169 effect on neutralization, while seven ($R57G_{HC}$, $T98R_{HC}$, $Y110G_{HC}$, $Y27S_{LC}$, $Y48L_{LC}$, $F93Y_{LC}$,
170 $C101F_{LC}$) significantly affected the breadth and potency of the resulting DH270min1 mutants
171 (Figure 2A). Based on these results, two other minimized antibody variants, DH270min11, which

172 combined the 12 mutations that had some effect on antibody breadth, and DH270min12, which
173 preserved only the seven acquired mutations most critical for function, were developed and
174 experimentally characterized. Compared to DH270.6 and DH270min1, these antibodies were
175 less broad and potent on the same panel of 15 DH270.6-sensitive viruses used in the previous
176 experiments (Figure 2A). To further assess the minimized DH270.6 variants, neutralization was
177 also measured on a multi-clade panel of 208 viral isolates. DH270.6 was previously shown to
178 neutralize 114 viruses from the global panel with a mean IC_{50} of 0.136μg/ml (Bonsignori et al.,
179 2017a). In comparison, DH270min1 neutralized 100 viruses (mean IC_{50}=0.113μg/ml),
180 DH270min11 neutralized 99 viruses (mean IC_{50}=0.135μg/ml) and DH270min12 neutralized 68
181 viruses (mean IC_{50}=0.408μg/ml) (Figure 2B, Supplementary Figure 2). Therefore, DH270min11,
182 which contained only 12 of the 42 acquired mutations, recapitulated 90% of the breadth of
183 DH270.6, revealing that only a small subset of all DH270.6 acquired mutations is required for
184 the development of the antibody into its broadly neutralizing form. Nine of the 12 mutations in
185 DH270min11 ($G31D_{HC}$, $S55T_{HC}$, $G57R_{HC}$, $R98T_{HC}$, $G110Y_{HC,}$ $S27Y_{LC}$, $L48Y_{LC}$, $Y93F_{LC}$, $S97A_{LC}$)
186 interact with the three components of the glycan-V3 epitope, the base of the V3 loop and the
187 glycans at positions 301 and 332, while three mutations are located away from the paratope and
188 likely contribute to the stability and conformation of the antibody (Figure 2C). While improbable
189 mutations make up 33% of the total mutations acquired by DH270.6, they represent 83% (10
190 out of 12) of those maintained in DH270min11. Taken together these results demonstrate that
191 only a small fraction (28%) of the mutations acquired by DH270.6 are required for its breadth
192 and potency. However, the majority of the functionally critical mutations are predicted to occur
193 with low probability during DH270.6 development and may restrict the development of this
194 lineage *in vivo*.

195 **Identification of molecules that preferentially bind antibodies containing the**
196 **DH270min functional mutations.** DH270min11 offers a significantly shorter evolutionary

197 pathway to elicit DH270.6-like antibodies. To identify boosting candidate immunogens that can
198 elicit similar bnAbs, we aimed to find molecules that preferentially interact with the key acquired
199 mutations in DH270min11. We reasoned that molecules that engage residues critical for
200 DH270.6 breadth *in vitro* may elicit antibodies with those target residues by vaccination, as was
201 previously demonstrated for the induction of DH270.6-like precursor antibodies containing the
202 acquired mutations $R57_{HC}$ and $T98_{HC}$ by the DH270 lineage activating immunogen 10.17DT
203 (Saunders et al., 2019). To further mature these immune responses to breadth, boosting
204 immunogens will be required to select additional mutations contained in DH270min11.

205 We previously isolated multiple HIV quasispecies that developed in subject CH848 in
206 whom the DH270.6 V3-glycan B cell lineage arose (Bonsignori et al., 2017a). We measured the
207 ELISA binding of recombinantly expressed CH848 gp120s derived from 96 Envs in this panel to
208 DH270min1 and to mutated antibodies where each residue maintained from DH270.6 was
209 reverted to its UCA identity (Figure 3, Supplementary Figure 3). The "selection strength" of each
210 gp120 for an acquired mutation present in DH270min1 was determined by comparing its
211 DH270min1 binding to its interaction with a DH270min1 antibody containing the UCA mutation
212 at the site of interest. The calculated fold decrease in binding indicated the degree to which a
213 potential immunogen engages a respective DH270min1 acquired mutation; we predict that
214 molecules that preferentially interact with a given antibody residue *in vitro* are promising
215 candidate immunogens to engage and expand antibodies that developed the same amino acid
216 mutation *in vivo*.

217 From this panel, we identified molecules that preferentially interacted with eight of the
218 twelve DH270.6 acquired mutations present in DH270min11, and six of the seven mutations
219 present in DH270min12 (Figure 3, Supplementary Figure 3). Multiple gp120s preferentially
220 bound the antibody through the key acquired mutations $R57_{HC}$, $T98_{HC}$, $Y110_{HC}$, $Y27_{LC}$ and
221 $Y48_{LC}$, while no gp120 selectively interacted with mutations at positions 31_{HC}, 51_{HC}, 55_{HC} and

222 101_{LC}. Previously, a vaccination regimen made of sequential immunizations with Envs 10.17,
223 836.31, 358.06, 1432.41, and 526.02 was proposed for the elicitation of DH270.6-like antibodies
224 (Bonsignori et al., 2017a). These immunogens were chosen based on their predicted ability to
225 select for the $G57R_{HC}$ improbable mutation and because they have progressively longer V1
226 loops. These immunogens were included in this analysis and revealed that five out of the six
227 molecules showed strong selection for at least three mutations (Figure 3B). As a group, this
228 immunogen panel preferentially engaged 9 out of the 12 acquired mutations in DH270min11
229 (Figure 3B, Supplementary Figure 3). However, our results indicate that more efficient
230 sequential vaccination regimens that use a subset of these previously proposed molecules
231 combined with newly identified ones could be developed based on our new criteria. In addition
232 to the engagement of specific mutations, the overall affinity of an immunogen for a target
233 antibody is also critical (Abbott et al., 2018). Both 836.31 and 1432.41 have a similar mutational
234 selection profile, but 1432.41 has a significantly higher binding for DH270min1 (Supplementary
235 Figures 3 and 4), which recommends its use over 836.31. While 526.02 showed strong
236 selection for a large number of the targeted mutations, its overall affinity for DH270min1 was
237 found to be low (Supplementary Figure 4). However, our analysis identified another molecule,
238 526.09, that had a comparable mutational profile, but a significantly higher affinity for
239 DH270min11 (Supplementary Figure 4). The “minimized” DH270 can therefore be leveraged to
240 identify molecules that preferentially interact with the key functional mutations of DH270.6.

241 **Characterization of Envs that bind antibodies with multiple DH270min acquired**
242 **mutations**. In the single mutant DH270min1 antibody screen, we evaluated gp120 molecules
243 for their ability to interact with one critical mutation at a time. However, in a vaccination scenario,
244 immunogens will interact with diverse BCRs that contain various amino acids at multiple sites in
245 the binding interface. To drive activated DH270.6 precursors to breadth, candidate immunogens
246 need to preferentially select from this diverse BCR repertoire the ones that contain the key

247 DH270.6 amino acids identified in DH270min1. One way to assess this at the vaccine design
248 stage is to ensure that selected immunogens preferentially interact with antibodies containing
249 the DH270.6 amino acids over the ones present in the unmutated common ancestor (UCA). To
250 predict the ability of our selected molecules to achieve this goal *in vivo*, we established an *in*
251 *vitro* approach that employs high throughput screening of single-chain variable fragment (scFv)
252 libraries displayed on the surface of yeast (Chao et al., 2006). A library was developed that
253 contains all the possible scFv variants of DH270min1 with either the amino acid present in the
254 UCA or in DH270.6 at each mutated amino acid position (Figure 4A). Therefore, this library
255 represents a subset of the possible evolutionary paths of the DH270UCA towards DH270min1.
256 The library was sorted by FACS for binding to five different envelopes: the germline targeting
257 immunogen 10.17DT and 1432.41, 836.31, 358.06, and 526.02 identified above (Figure 4B).
258 While gp120s were used for immunogen identification above due to their availability and ease of
259 production (Figure 3), candidate immunogens will be expressed as SOSIP Envs for
260 immunizations and were therefore used in this format for library screening. The sequences of
261 the selected scFvs bound by each envelope were isolated and analyzed by next generation
262 sequencing. The frequency of the “mature” DH270.6 amino acids across the selected clones at
263 each target site was compared to the frequency of that mutation in the naïve library in order to
264 determine the “enrichment levels” at a given site for the DH270.6 amino acid over the one from
265 the UCA (Figure 4C). To validate this approach, we first compared the enrichment of amino
266 acids selected from the scFv library by sorting with a given envelope to the presence of the
267 same mutations in antibodies elicited by vaccination with the respective molecule. The only
268 available data set for this analysis comes from 10.17DT, which was previously used to
269 immunize DH270UCA knock-in mice and the heavy chain diversity of the antibody repertoire
270 induced by vaccination was described in detail by next generation sequencing (Saunders et al.,
271 2019). The enrichment of a given amino acid at a site in the heavy chain of 10.17DT elicited
272 antibodies was determined by computing the ratio of the experimentally observed versus the

273 computationally expected frequency for that amino acid with ARMADiLLO (Wiehe et al., 2018).
274 Enrichment of a given DH270.6 amino acid from the scFv library correlated well with the
275 observed frequency of that same residue in vaccine elicited antibodies (R^2= 0.625 over 9
276 positions analyzed) (Figure 4D, Supplementary Figure 5). Therefore, our scFv library screening
277 approach can describe, at least qualitatively, the ability of a given envelope to elicit DH270.6-
278 derived antibodies with target functional mutations.

279 Library selection and sequence analysis revealed that, taken as a group, 10.17DT,
280 1432.41 and 358.06 favored the mature over the UCA amino acids at all the key positions in
281 DH270min11, with the exception of 31_{HC}, 51_{HC} and 93_{LC} (enrichment levels>10%). The acquired
282 mutations at position 31_{HC} and 93_{LC} are probable and expected to occur with high frequency *in*
283 *vivo*, which should facilitate their selection; indeed, significant levels of $D31_{HC}$ are observed in
284 the repertoire of DH270UCA knock-in mice vaccinated with 10.17DT (Saunders et al., 2019).
285 The sequence of 10.17DT, 1432.41 and 358.06 envelopes may present an “affinity gradient” for
286 the selection of key amino acids at positions 55_{HC}, 57_{HC}, 98_{HC}, 110_{HC}, 94_{LC}, 97_{LC}, 101_{LC}, based
287 on the progressively higher enrichment levels observed for the target amino acids in the library
288 clones selected with these three Envs. However, for the robust induction of antibodies with the
289 full breadth of DH270.6, our results suggest that additional immunogens will likely be needed to
290 more strongly select for key improbable mutations $M51_{HC}$, $Y27_{LC}$ and $L48_{LC}$. The scFv library
291 was also labeled with 526.02, but only a small number (<0.1%) of clones showed binding above
292 background, which impeded sequence analysis (data not shown). These data, corroborated by
293 the weak binding of 526.02 to DH270min1 (Supplementary Figure 4), suggest that 526.02 only
294 interacts with DH270.6-derived antibodies that already contain the majority of the functional
295 mutations required for breadth, and further supports the use of the alternative envelope 526.09
296 as a final “boost”. Taken together, the scFv library screens showed that the sequence of

envelopes composed of 1432.41, 358.06 and 526.09 can preferentially select for antibodies containing the majority of the acquired mutations present in DH270.6-like bnAbs.

Identification of alternative Env recognition modes by minimized DH270.6 antibodies. The significant number of functional improbable mutations in DH270.6 likely represents a barrier for the induction of similar antibodies by vaccination. While envelopes can be identified that engage DH270.6-derived antibodies with these rarely occurring amino acids as shown above, it would be advantageous to discover alternative developmental pathways of DH270.6-like bnAbs that may occur with higher frequency *in vivo* and may be easier to replicate by vaccination. Combinations of more probable amino acids, not observed during natural evolution, may exist at the key positions in DH270min11 resulting in antibodies with alternative sequences that maintain broad neutralization.

To investigate this possibility, we aimed to identify DH270min11 variants that contain alternative amino acids at the paratope positions involved in the recognition of the V3 loop. Three improbable acquired amino acids, including Arg at position 57 that is critical for the development of DH270.6 breadth (Bonsignori et al., 2017b; Saunders et al., 2019), interact with the base of the V3 loop in DH20min11. A library was constructed that sampled all the possible combinations of amino acids at these sites (55_{HC}, 57_{HC}, and 97_{LC}) as well as full diversity at position 51_{HC} that was judged to contribute second-shell packing interaction to three paratope residues that directly contact the Env (Figure 5A). By sampling multiple DH270min11 improbable residues that have the same functional role, i.e. V3 loop binding, our goal was to thoroughly search for alternative Env recognition modes that rely on more probable amino acids. The resulting library of DH270min11 scFv variants was sorted in succession for binding to SOSIP Envs that were identified above (10.17DT, 358.06, and 1432.41 twice) (Figure 5B). Pseudoviruses with Envs from this panel are progressively harder to neutralize by DH270.6 and by antibodies from the same lineage that appeared earlier in the development, with 10.17DT

322 being the easiest to neutralize (Supplementary Figure 6). Therefore, successive selections of
323 the scFv library with these envelopes should identify antibody sequences with increasing
324 breadth for difficult to neutralize viruses.

325 Clones selected by one Env were collected, expanded and subjected to additional sorts
326 with the next molecules in the panel (Figure 5B). The DNA of clones bound by 10.17DT and
327 1432.41 was isolated and analyzed with PacBio long read sequencing technology to identify the
328 full-length sequence of selected scFv variants. As expected, the overall sequence diversity of
329 the isolated clones was reduced from one round of selection to the next, since fewer amino acid
330 variants are expected to be tolerated in antibodies that bind the Envs of harder to neutralize
331 viruses. Of note, after the last selection, the clones present with the highest frequency contained
332 combinations of amino acids at the DH270min11 sites involved in V3 loop recognition that are
333 not present in either the DH270.6 or its UCA (Figure 5C). Using ARMADiLLO analysis (Wiehe et
334 al., 2018), multiple newly identified amino acids were predicted to occur with higher probability
335 *in vivo* than those naturally present in DH270.6. In particular alanine at position 57, which is
336 expected to occur four times more frequently than the native Arg, was found to be enriched in
337 the majority of the selected clones. This indicated that DH270.6-related broadly neutralizing
338 antibodies may exist that have diverse and more probable amino acids that those present in the
339 native bnAb.

340 To confirm this, two DH270min11 variants identified from the library, named AltMinV3_1
341 and AltMinV3_2, were expressed recombinantly and characterized. AltMinV3_1 contained the
342 sequence of the most frequent clone present at the end of the selection rounds, whereas
343 AltMinV3_2 contained more probable amino acids at all the four V3 loop interaction positions
344 sampled in the library. While their breadth was reduced compared to DH270min11, AltMinV3_1
345 and AltMinV3_2 still displayed significant breadth; they neutralized 10 and 7 viruses respectively
346 from the panel of 15 DH270.6-sensitive isolates employed above (Figure 5D). Taken together,

347 these results show that diverse amino acids can exist at the key DH270.6 paratope sites that
348 occur with higher probability *in vivo* and that are functionally similar to the native residues.
349 Therefore, multiple, more accessible pathways than the one naturally observed may exist to
350 induce DH270.6-like antibodies by vaccination. Such pathways may be induced by the
351 candidate immunogens identified here, as evidenced by the ability of these SOSIPs to select for
352 DH270.6-like antibodies that have significant breadth, but that contain more probable acquired
353 mutations in the paratope.

354 Discussion

355 A major task of current HIV vaccine development efforts is to design successful
356 sequential immunogen regimens capable of binding to B cell receptors of bnAb lineage
357 members that have functional improbable mutations required for potent bnAb activity. Here we
358 report a rapid strategy for identification of the minimal functional mutations needed for antibody
359 breadth and the identification of HIV Envs as sequential immunogen candidates that bind to
360 bnAb lineage BCRs. Our results show that only a small number of acquired mutations are
361 necessary for the development of DH270.6 V3-glycan bnAb precursors into broadly neutralizing
362 antibodies. Twelve amino acid changes from UCA were sufficient to recapitulate 90% of
363 DH270.6 neutralization. While the majority of these mutations were located in the paratope,
364 three of them did not directly contact HIV Env. Therefore, residues away from the binding site
365 also modulate function, likely by affecting the antibody conformation or stability (Klein et al.,
366 2013). Indeed, DH270min3, which contained only the acquired mutations in the paratope,
367 displayed only 66% of the breadth of the mature bnAb. These results are in line with those
368 reported for BG18, another HIV bnAb that targets the same glycan-V3 epitope, but uses a
369 different binding orientation and develops from other germline genes (Barnes et al., 2018).
370 Recently, a “minimized” BG18 was described that preserves 22 out of the 60 acquired mutations
371 and recapitulates 66% of the neutralization breadth of the mature bnAb (Steichen et al., 2019).

372 minBG18 contains only the acquired mutations located at the binding interface, while all the
373 amino acids located away from the paratope are reverted to their UCA identity. In comparison,
374 by considering acquired mutations outside the binding interface in our designs, DH270min11
375 almost fully recapitulates the breadth of DH270.6, while maintaining a lower percentage (28%)
376 of the total acquired mutations than minBG18 (36%). VRC01, a bnAb that targets the CD4
377 binding site on Env, was the first bnAb to be "minimized". minVRC01 retained 93% of the
378 mature VRC01 breadth by preserving 24 out of 65 acquired mutations together with a three
379 amino acid deletion in the CDR L1 loop of the inferred UCA (Jardine et al., 2016). minVRC01
380 was developed by screening 4 different scFv libraries that sampled UCA and mature amino
381 acids for over 20 selection rounds (Jardine et al., 2016). Compared to this experimentally
382 intensive approach, our strategy relied on computational and structural analysis in order to
383 determine the residues critical for the neutralization function of DH270.6 more rapidly and at a
384 significantly reduced cost. Amino acids that contact the HIV Env were identified from available
385 structural data (Fera et al., 2018; Saunders et al., 2019), while residues located away from the
386 interface critical for broad neutralizing function were determined by computational modeling.
387 This approach identified a subset of 17 out of 42 acquired mutations that recapitulated almost all
388 of the DH270.6 breadth; subsequent single site mutagenesis studies reduced this subset to 12
389 mutations in DH270min11. Our combined computational and experimental approach can
390 therefore efficiently identify functionally important residues that occur during antibody
391 development, and should be broadly applicable to the study of other heavily mutated bnAbs.

392 Of the 12 acquired mutations present in the minimized DH270.6, 10 were improbable
393 based on computational predictions that estimate the propensity of AID to mutate the antibody
394 gene regions where they are located (Wiehe et al., 2018). HIV bnAbs are enriched for
395 improbable mutations and such mutations have been shown to have important functional roles
396 across different antibodies (Bonsignori et al., 2016; Shen et al., 2020). Forty-six percent of the

397 acquired mutations maintained in the minVRC01 antibody and 28% of those in minBG18 are
398 improbable. In comparison, while improbable changes constitute 33% of the acquired mutations
399 in the DH270.6, 83% of the amino acids maintained in DH270min11 are improbable, highlighting
400 the functional importance of these rarely occurring sequence changes for the breadth
401 development. This conclusion is further supported by our data showing that a DH270.6-derived
402 antibody, DH270Prob, containing only the naturally acquired probable mutations had no
403 neutralization ability (Fig 1C). Since only a small number of sequence changes, but no
404 insertions or deletions, are required for the development of DH270.6-like bnAbs from germline
405 precursors, these antibodies are an attractive target for elicitation by vaccination. DH270min11
406 is only 8% mutated from the DH270UCA, and represents to our knowledge one of the least
407 mutated HIV antibodies with broadly neutralizing capabilities (Simonich et al., 2016).

408 While DH270min11 should be easier to induce by vaccination than DH270.6, the
409 presence of a large number of improbable mutations may present a significant barrier for its
410 elicitation. However, alternative amino acids with similar functional properties that occur with
411 higher frequency *in vivo*, may exist at the sites containing improbable acquired mutations.
412 Indeed, we found this to be the case for four DH270min11 sites that contain improbable amino
413 acids and that are involved in interactions with the Env V3 loop. Using high throughput library
414 screening, non-native, more probable amino acids were found at all four sites including position
415 57 which is critical for breadth development. Two tested DH270min11 antibodies containing
416 such alternative paratope sequences maintained significant neutralization breadth, although
417 their activity was more restricted than that of DH270min11 or DH270.6. Broader and more
418 potent bnAbs may be isolated by subjecting the same scFv library to additional selection rounds
419 with Envs from viruses that are more resistant to DH270.6. Nevertheless, the elicitation of a
420 strong polyclonal response that targets the glycan-V3 epitope may provide sufficient protection,
421 even though the individual monoclonal antibodies are not as broad or potent as DH270.6. Our

422 library screening experiments indicate that such bnAbs with diverse paratope sequence,
423 containing amino acids predicted to occur frequently *in vivo,* are selected *in vitro* by the
424 candidate immunogens identified here. These results further highlight the potential of our
425 proposed vaccination regimen to induce DH270.6-like bnAbs through diverse developmental
426 pathways that are more likely to arise naturally.

427 Compared to previous HIV bnAb minimization studies, we leveraged our minimized
428 DH270 antibodies to find and characterize envelopes for the induction of similar antibodies by
429 vaccination. Our approach relied on the identification of proteins that preferentially interacted
430 with DH270.6-derived antibodies through mutations deemed essential for function. Diverse
431 molecular properties can control the ability of candidate immunogens to contact different
432 DH270min11 acquired mutations. The size and branching of glycans present at positions N301
433 and N332 can have a significant effect on antibody recognition. These glycans are variable
434 across different Envs and their processing is affected by the presence of neighboring
435 glycosylation sites, for example, those that may exist at the tip of the V1 loop (Cao et al., 2017;
436 Saunders et al., 2019; Struwe et al., 2018). In addition, sequence variation in the V3 loop can
437 also affect molecular contacts with the acquired mutations. Envelopes were chosen from a
438 panel of molecules previously selected from the patient who gave rise to the DH270 lineage
439 (Bonsignori et al., 2017a), based on their ability to differentially bind to minimized antibodies that
440 either contain or lack a target mutation. Chosen envelopes were further tested in a high
441 throughput fashion for their ability to select antibodies containing multiple DH270min11 acquired
442 mutations *in vitro*. Characterization of diverse molecules in this fashion can rationally and rapidly
443 identify candidate immunogens towards the elicitation of antibodies containing key acquired
444 mutations *in vivo*. With this approach we identified Envs hypothesized to select for DH270.6-like
445 bnAbs that contain all but one of the acquired improbable mutations in DH270min11 (Figure 6).
446 In order to more robustly select for the improbable acquired mutations $M51_{HC}$, $Y27_{LC}$ and $L48_{LC}$,

447 additional boosting immunogens may be required. Based on one available data set (Saunders
448 et al., 2019), DH270min11 residues selected from the antibody libraries by the 10.17DT
449 immunogen correlated well with amino acids present at the same positions in antibodies elicited
450 by 10.17DT immunizations. Nevertheless, elicitation of antibodies *in vivo* depends on many
451 factors beyond binding affinity that are not captured in our *in vitro* characterization. For example,
452 precursor frequency and their ability to be recruited into germinal centers by different
453 immunizations together with the stimulation of T helper cells will be essential for the success of
454 this vaccination regimen. (Abbott et al., 2018; Lee et al., 2020; Mesin et al., 2020). Therefore,
455 the envelope discovery and characterization approach presented here is primarily meant to
456 provide a rational way to classify and prioritize candidate immunogens for *in vivo* testing. The
457 potential of the vaccination regimen identified here to induce DH270.6-like bnAbs that contain
458 the key target mutations *in vivo* will be assessed in animal models in upcoming work.

459 HIV vaccine boosting regimens have typically been determined empirically and usually
460 involve serial immunizations with molecules that progressively resemble the native HIV Env
461 (Dosenovic et al., 2015a; Escolano et al., 2016; Sanders et al., 2015; Steichen et al., 2016; Tian
462 et al., 2016). With the exception of one study that started with a later stage bnAb precursor and
463 used sera screening and B cell repertoire analysis to inform immunogen choice (Escolano et al.,
464 2016), such boosting regimens had limited success in maturing activated bnAb precursors
465 (Briney et al., 2016; Dosenovic et al., 2015a). Our approach aims to rationally identify and
466 validate Envs that specifically bind to bnAb antibody lineage members bearing functional
467 improbable mutations. Similar library platforms to the one described here for DH270.6 can be
468 developed for other HIV bnAbs, in order to identify sequential Envs that target bnAb lineages
469 that contain rare mutations necessary for HIV neutralization breadth. In conclusion, this study
470 describes a rational and efficient method to determine the key amino acids required for antibody

471 function, and establishes a generalizable approach to identify candidate envelope immunogens
472 for vaccine studies.

473 Methods

474 **Computational identification of functionally critical acquired mutations.**
475 Computational design of minimally mutated DH270.6 antibodies were based on the crystal
476 structure of the DH270.6 scFv in complex with Man9-V3 glycopeptide (PDB: 6CBP), a
477 previously described synthetic peptide that mimics the glycan-V3 epitope on Env (Alam et al.,
478 2017; Fera et al., 2018). Based on structural analysis, different subsets of amino acids were
479 identified that were deemed not important for DH270.6 stability or binding. The amino acids at
480 these sites were changed to their UCA identity and the Rosetta energy of the new antibodies
481 was computed. Upon reversion to UCA, 5000 Rosetta models were generated for each
482 "minimized" antibody decoys by sampling all amino acid side chains and allowing fine backbone
483 movement (Supplementary Figure 1) (Lauck et al., 2010). Antibodies with decoys that sampled
484 Rosetta free energy levels on par with those of the mature DH270.6 were selected for
485 experimental characterization (Supplementary Figure 1).

486 **Plasmids and DNA synthesis.** DNA for yeast display libraries was synthesized as a
487 pooled oligo library by BioXp (CodexDNA). Genes encoding the antibody heavy and light chains
488 were commercially synthesized and cloned into pcDNA3.1 vector (GenScript). DNA primers for
489 sequencing and insert amplification were ordered from IDT.

490 **Development and screening on scFv libraries on the surface of yeast.** *Library*
491 *design and synthesis.* DH270min1 sites with amino acids maintained from DH270.6 (heavy
492 chain: G31D, Y32F, I51M, N54Q, S55T, G57R, R98T, G110Y; light chain: S26K, S27Y, Y32H,
493 L48Y, Y60T, Y93F, A94G, S97A, F101C) were allowed to sample either the mature DH270.6 or
494 the germline DH270UCA3 residue in an all against all fashion (library size of 1.31x10^5 scFv

495 variants). Library DNA was synthesized as a pooled oligo library by BioXp and amplified with
496 High Fidelity Phusion polymerase (New England Biolabs). PCR products were gel extracted
497 (Qiagen Gel Extraction kit) to select full length genes that were further purified (Qiagen PCR
498 cleanup kit) as per the manufacturer's protocol. The V3 loop library that aimed to identify
499 alternative amino acids at the functional sites in DH270min11 maintained from DH270.6, tested
500 all the possible amino acids combinations as follows: (heavy chain: M51, T55, R57; light chain:
501 A97).

502 *Library transformation into S. Cerevisae*. Libraries were generated to display DH270.6
503 scFv variants on the surface of yeast as previously described (Benatuil et al., 2010; Chao et al.,
504 2006). *S. cerevisiae* EBY100 cells were transformed by electroporation with a 3:1 ratio of 12µg
505 scFv library DNA and 4µg pCTCON2 plasmid digested with BamHI, SalI, NheI (New England
506 Biolabs). The typical sizes of the transformed libraries, determined by serial dilution on selective
507 plates, ranged from 1-5x10^7. Around 70-90% of the sequences recovered from the transformed
508 libraries were confirmed to contain full length, in-frame genes by Sanger sequencing. Yeast
509 Libraries were grown in SDCAA media (Teknova) with Pen-Strep at 30C and 225 rpm.

510 *Library screening by FACS.* scFv expression on the surface of yeast was induced by
511 culturing the libraries in SGCAA (Teknova) media at a density of 1x10^7 cells/mL for 24-36
512 hours. Cells were washed twice in ice cold PBSA (0.01M sodium phosphate, pH 7.4, 0.137M
513 sodium chloride, 1g/L bovine serum albumin) and labeled with biotinylated SOSIP Envs (10.17
514 and 10.17DT) at a concentration of 300nM and incubated for 1hr at 4C. Cells were then washed
515 twice with PBSA and resuspended in secondary labeling reagent 1:100 α c-myc:FITC (ICL) and
516 1:20 streptavidin:R-PE (Sigma-Aldrich) and incubated at 4C for 30 minutes. Cells were washed
517 twice with PBSA after incubation with the fluorescently labeled probes and sorted on a BD
518 FACS-DiVa. Double positive cells for PE and FITC were collected and expanded for one week
519 in SDCAA media supplemented with pen-strep before successive rounds of enrichment. Sorts

520 of the libraries with non-biotinylated SOSIPs (358.06, 1432.41, 836.31 and 0526.02) used 4-fold
521 excess PGT151 mAb and 1:60 α-hIgG:PE (Invitrogen) pre-incubated for 60 minutes as the
522 phycoerythrin signal. The *DH270min1 library* was screened separately for binding of SOSIPs
523 10.17DT, 10.17, 1432.41, 358.06, 526.02, 836.31. The *DH270min11 V3 loop library* was sorted
524 sequentially with SOSIPS 1017.DT, 358.06, and 1432.41 twice. FACS data was analyzed with
525 Flowjo_v10.6 software (Becton, Dickinson & Company). All clones by FACS were expanded,
526 and their DNA was extracted (Zymo Research) for analysis by Next Generation Sequencing and
527 Sanger sequencing analysis (Genewiz).

528 **Sequence analysis of library clones.** scFv encoding plasmids were recovered from
529 yeast cultures by yeast miniprep with the Zymoprep yeast plasmid miniprep II kit (Zymo
530 Research). Isolated DNA was transformed into NEB5α strain of *E. coli* (New England Biolabs)
531 and the DNA of individual bacterial colonies was isolated (Wizard Plus SV Minipreps, Promega)
532 and analyzed by Sanger sequencing to confirm the validity of the FACS selections. To prepare
533 plasmids for Next Generation Sequencing, the scFv containing region from isolated plasmids
534 was amplified by PCR using Q5 high fidelity PCR (NEB). Illumina NGS samples were prepped
535 and run using the Illumina MiSeq v3 reagent kit following manufacturer's protocols pooling four
536 library samples per lane. Illumina sequencing returned an average of 14.3 million reads per
537 sample, of which an average of 13.1 million mapped to the scFv amplicon.

538 PacBio long read NGS was completed by Genewiz pooling 3-4 library samples per SMRT cell.
539 Sequencing results by PacBio returned 35-47k reads per sample sequenced, of which 15-26k
540 aligned to the scFv amplicon. Sequencing data was processed using Geneious Prime and
541 programs developed in-house to compute the amino acid frequency and distribution.

542 **Antibody expression and purification.** Antibodies were expressed and purified as
543 previously described (Saunders et al., 2019). Briefly, 100mL cultures of Expi293F cells at a
544 density of 2.5×10^6 cells/mL were transiently transfected with 50μg each heavy and light chain

545 encoding plasmids and Expifectamine (Invitrogen) per manufacturer's protocol. Five days after
546 transfection, cell culture media was cleared of cells by centrifugation, and the supernatant was
547 filtered with 0.8 micron filters. Clarified supernatant was incubated with Protein A beads
548 (ThermoFisher) over night at 4C, washed with 20mM Tris supplemented with 350mM NaCl
549 (pH=7), followed by elution with a 2.5% Glacial Acetic Acid Elution Buffer and subsequent buffer
550 exchange into 25mM Citric Acid supplemented with125mM NaCl (pH=6). IgG expression was
551 confirmed by reducing SDS-PAGE analysis, and quantified by measuring absorbance at 280nM
552 (Nanodrop 2000)

553 **Recombinant HIV Env production.** SOSIP envelopes were produced recombinantly as
554 previously described (Saunders et al., 2019). Briefly, Freestyle 293 cells were transfected with
555 293Fectin complexed with envelope-expressing DNA and furin-expressing plasmid DNA. After 6
556 days, SOSIPS were purified via PGT145 affinity chromatography with subsequent size
557 exclusion chromatography. Trimeric HIV-1 Env fractions were pooled, snap-frozen, and stored
558 at -80C in 10mM Tris pH 8, 500mM NaCl buffer. Expression of gp120 proteins occurred as
559 previously described in 293F cells by transient transfection with 293Fectin (Invitrogen) and
560 purification by metal affinity and Size Exclusion Chromatography (Alam et al., 2013; Liao et
561 al., 2013a; Liao et al., 2006)

562 **Pseudovirus neutralization assay.** Neutralization of antibodies was measured in TZM-
563 bl cells in a 96 or 384-well plate format assay using either a 20-virus panel comprised of viruses
564 known to be sensitive to DH270.6, or on a 208 Env-pseudovirus panel representative of the
565 major genetic subtypes of circulating virus (Bonsignori et al., 2017a; Bonsignori et al., 2016).
566 Signal was calculated as a reduction in luminescence compared to control wells and reported as
567 IC50 in μg/mL.

568 **ELISA Assay.** Direct-binding ELISAs were performed as described on 96 gp120
569 molecules isolated previously (Bonsignori et al., 2017a; Bonsignori et al., 2016). 384-well plates
570 were blocked overnight at 4C. Starting concentrations of 100ug/mL purified antibody were
571 serially diluted 3-fold and incubated at room temperature for 1 hour. 1:30,000 HRP- conjugated
572 hIgG in assay diluent was added to plates, incubated for one hour, and developed using TMB
573 substrate. Plates were read at 450nm on a SpectraMax 384 PLUS reader (Molecular Devices).
574 (LogAUC).

575

576 **Acknowledgements.** We thank J. Baalwa, D. Ellenberger, F. Gao, B. Hahn, K. Hong, J. Kim, F.
577 McCutchan, D. Montefiori, L. Morris, E. Sanders-Buell, G. Shaw, R. Swanstrom, M. Thomson,
578 S. Tovanabutra, C. Williamson, and L. Zhang for contributing the HIV-1 envelope plasmids used
579 in the 208-strain panel. We thank K. McKee, C. Moore, S. O'Dell, G. Padilla, S.D. Schmidt, C.
580 Whittaker, and A.B. McDermott for assistance with neutralization assessments on the 208-strain
581 panel.

582

583

584

585

586

587

588

589

A

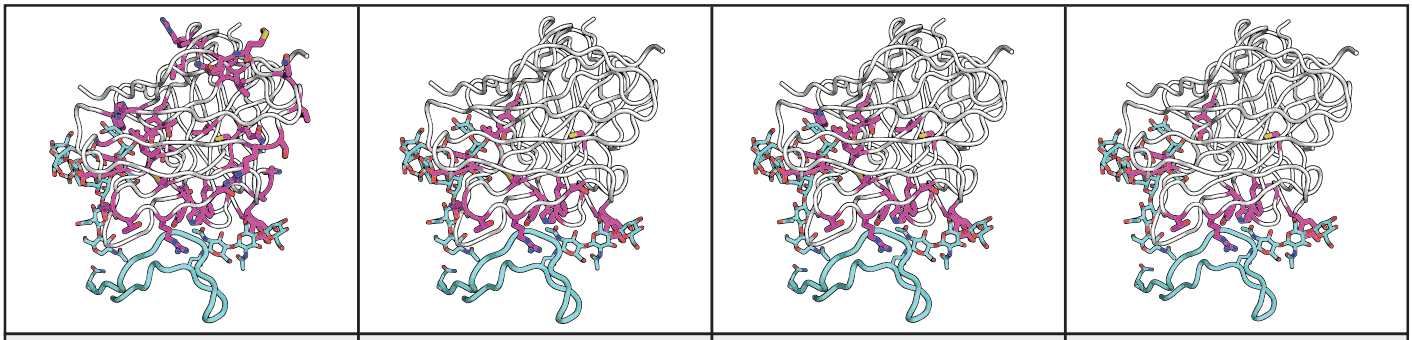

DH270.6	DH270min1	DH270min2	DH270min3
42 acquired mutations	17 mutations	20 mutations	12 mutations

B

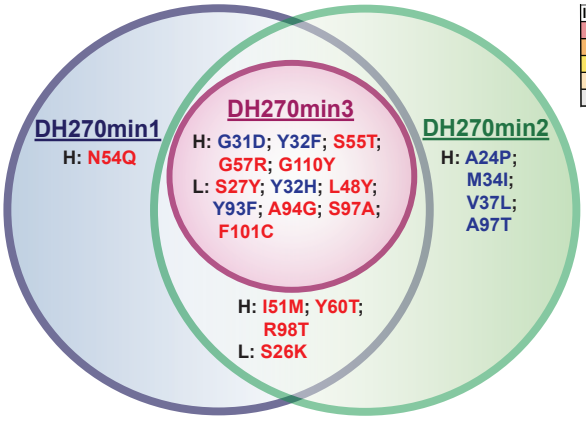

C

IC50 ug/ml
< 0.1
0.1 to 1
1 to 10
10 to 50
>50

	DH270.6	min1	min2	min3	Improb	Prob
92RW020	0.021	<0.023	<0.023	0.025	<0.023	>50
ZM55F.PB28a	0.03	<0.023	<0.023	0.585	0.041	>50
6101.10	0.04	<0.023	<0.023	0.12	<0.023	>50
JRFL	0.04	<0.023	<0.023	19.651	0.034	>50
ZM106F.PB9	0.05	<0.023	<0.023	0.096	<0.023	>50
DU156.12	0.07	0.068	0.078	0.989	0.158	>50
TRO.11	0.06	<0.023	<0.023	0.635	0.48	>50
DJ263.B	0.08	0.036	<0.023	10.882	1.43	>50
CAAN5342.a2	0.03	<0.023	<0.023	11.024	1.652	>50
DU422.1	0.19	0.192	0.202	3.776	0.315	>50
PVO.4	0.14	0.12	0.093	>50	34.477	>50
CNE58	0.28	0.166	0.074	>50	29.779	>50
TRJO4551.58	0.194	<0.023	<0.023	>50	>50	>50
DU172.17	0.27	0.258	0.303	>50	>50	>50
57128.vrc15	2	7.925	7.631	>50	>50	>50
Breadth	100.0%	100.0%	100.0%	66.7%	80.0%	0.0%
Potency	0.09	0.06	0.06	0.99	0.32	N/A
# AA Muts	45	17	20	12	14	28

Figure 1. Design of first generation minimized DH270.6 antibodies. A. Structural mapping of DH270.6 somatic mutations maintained in different DH270min variants. Mutations (magenta, sticks) were mapped on the structure of DH270.6 scFv (grey) in complex with an HIV Env derived V3-loop glycopeptide (cyan) (PDBID: 6cbp). Glycans at positions N301 and N332 are shown in sticks. **B.** Venn diagram of the acquired mutations present in the DH270min antibodies colored by their predicted in vivo probability (high=blue; low=red). **C.** Neutralization breadth and potency of DH270.6, DH270min antibodies, and DH270.6 variants that contain only the "probable" (DH270Prob) or "improbable" mutations (DH270Improb) on a panel of DH270.6 sensitive pseudoviruses. #AA Muts=the number of DH270.6 acquired mutations maintained in the respective antibodies.

A

Antibody	Virus ID										
	JRFL	DU156.12	TRO.11	DJ263.B	CAAN5342.a2	DU422.1	PAVO.4	CNE58	TRJO4551.58	DU172.17	57128.vrc15
DH270min1	<0.023	0.068	<0.023	0.036	<0.023	0.192	0.12	0.166	<0.023	0.258	7.925
HC.T60Y	<0.023	0.034	<0.023	0.113	<0.023	0.099	0.059	0.2	0.056	0.648	14.627
HC.Q54N	<0.023	0.028	<0.023	0.08	<0.023	0.088	0.085	0.183	0.106	2.068	46.365
LC.K26S	<0.023	<0.023	<0.023	0.137	<0.023	0.062	0.054	0.103	0.066	0.919	21.585
HC.F32Y	<0.023	0.033	<0.023	0.082	<0.023	0.092	0.05	0.132	0.073	0.675	14.712
LC.H32Y	<0.023	0.033	<0.023	0.045	<0.023	0.103	0.05	0.115	0.047	0.206	16.789
HC.D31G	<0.023	<0.023	<0.023	0.027	<0.023	0.061	0.059	0.163	<0.023	1.523	44.327
HC.M51I	<0.023	0.035	0.032	0.136	<0.023	0.118	0.071	0.157	0.102	2.164	>50
HC.T55S	<0.023	<0.023	<0.023	0.034	<0.023	0.104	<0.023	0.15	0.07	1.397	>50
LC.G94S	<0.023	0.028	<0.023	0.047	<0.023	0.125	0.071	0.156	0.577	9.465	>50
LC.A97S	<0.023	<0.023	<0.023	0.067	<0.023	0.161	0.581	0.269	0.584	49.97	>50
LC.C101F	<0.023	0.03	<0.023	0.035	<0.023	0.116	0.103	0.296	0.407	17.435	>50
LC.Y27S	<0.023	0.058	<0.023	0.118	<0.023	0.189	0.273	0.372	5.28	32.557	>50
LC.F93Y	0.025	0.049	<0.023	0.135	<0.023	0.192	0.602	0.592	9.848	>50	>50
HC.R57G	0.528	0.051	<0.023	0.901	0.038	0.205	1.635	5.303	>50	9.311	>50
LC.Y48L	0.086	0.143	0.05	0.46	<0.023	0.514	4.023	2.88	16.237	>50	>50
HC.T98R	1.397	0.183	0.117	1.167	<0.023	0.446	>50	13.37	>50	>50	>50
HC.Y110G	1.898	0.109	<0.023	0.58	2.987	0.502	>50	>50	>50	>50	>50
DH270min12	0.054	0.055	0.042	1.787	8.528	0.135	>50	23.14	27.04	>50	>50
DH270min11	<0.023	<0.023	0.026	0.116	<0.023	0.115	0.088	0.174	0.33	4.805	>50

B

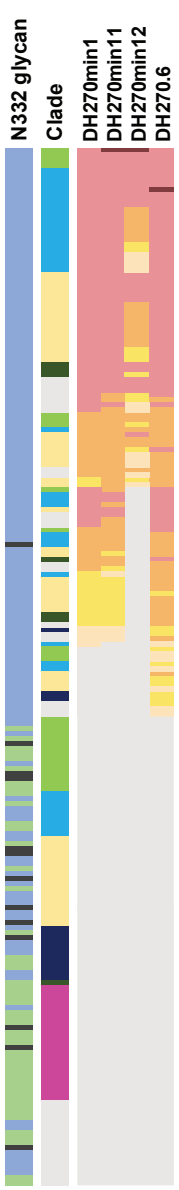

C

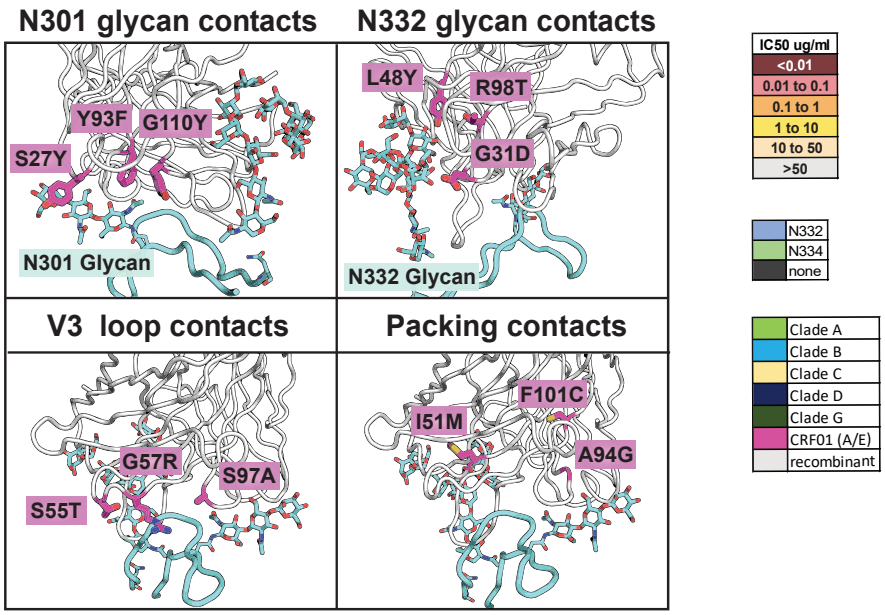

Figure 2. Additional minimization of DH270min1 by single site mutagenesis. A. The effect on neutralization of every DH270min1 acquired mutation assessed by single site mutagenesis to the corresponding UCA residue. Second generation minimized antibodies DH270min11 and DH270min12 contained only the acquired mutations important for DH270min1 neutralization. **B.** Neutralization breadth of minDH270 antibodies on a global panel of 208 pseudoviruses. **C.** Location and binding interactions of the DH270.6 acquired mutations (magenta, sticks) maintained in DH270min11.

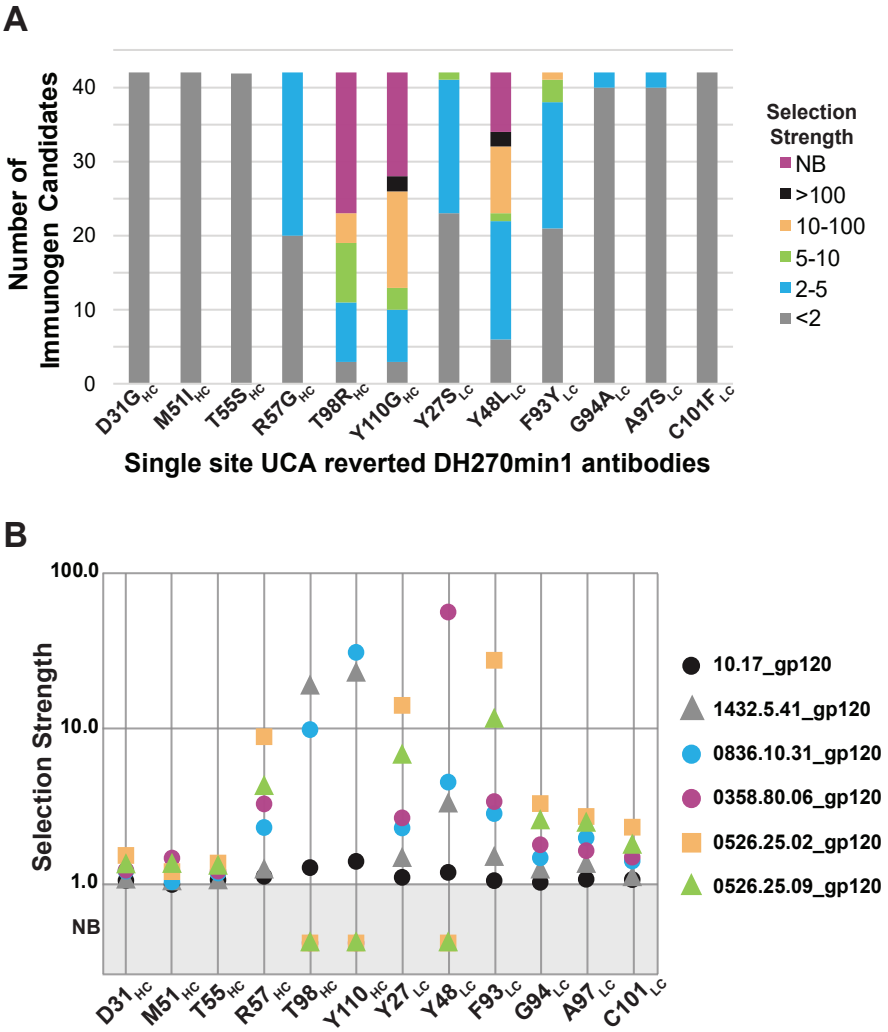

Figure 3. Identification of immunogen candidates that preferentially interact with DH270min1 through its acquired mutations. A. The number of tested gp120 immunogen candidates that preferentially interact with each of the acquired mutations in DH270min1. Only the acquired mutations present in DH270min11 are displayed. The top 50% gp120 molecules by DH270min1 affinity are shown. **B.** The selection strength of individual candidate immunogens for each of the acquired mutations present in DH270min11. NB=not binding.

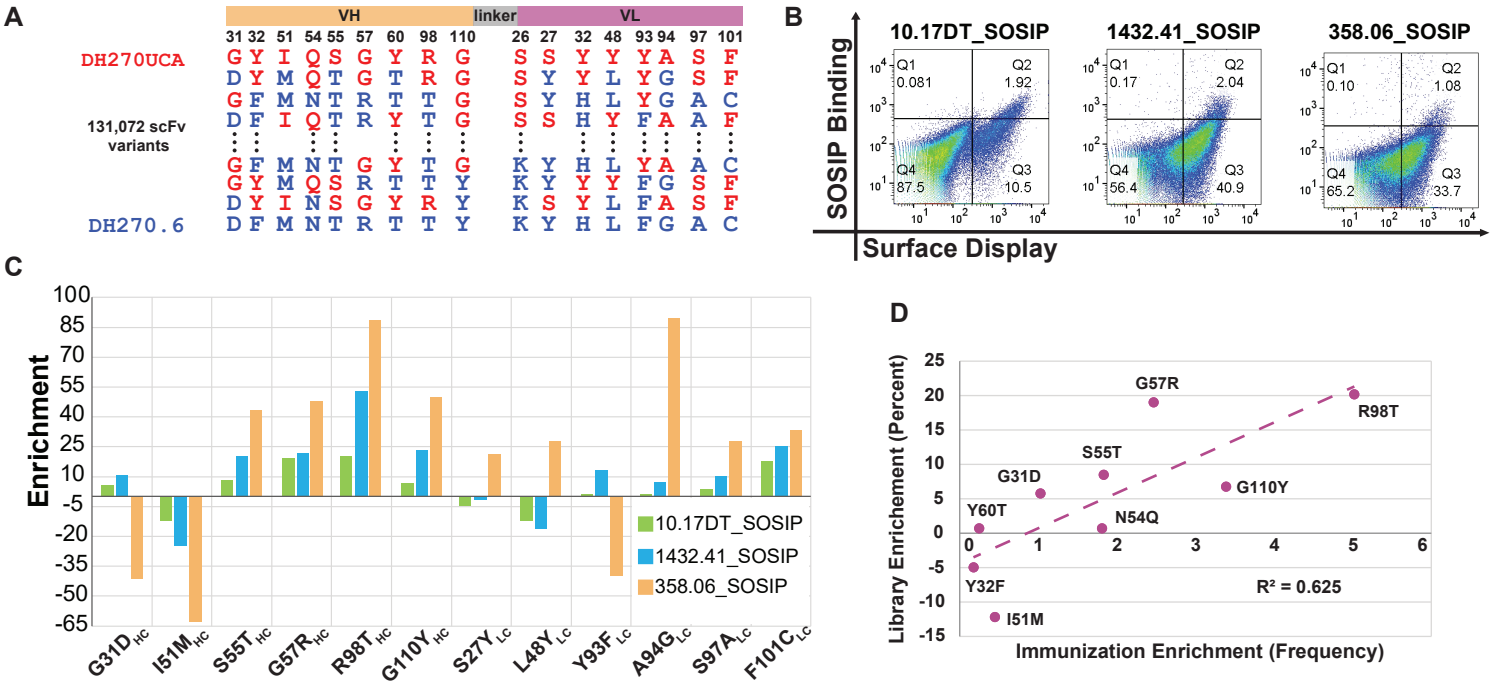

Figure 4. In vitro characterization of candidate immunogens towards selection of DH270.6-derived antibodies that contain the acquired mutations present in DH270min1. **A.** Design of a scFv library that sampled in combination each acquired mutation site in DH270min1. At each sampled position the amino acid present in the mature DH270.6 mAb (blue) or that found in the UCA (red) was randomly assorted. **B.** Selection of the scFv library for binding to different candidate immunogens by FACS. **C.** Enrichment levels of the acquired mutations in the clones isolated by the different immunogen candidates in **B,** computed relative to the frequency of the mutations in the unsorted library. Only the key acquired mutations present in DH270min11 are shown. **D.** The enrichment of mutations by vaccination, averaged from 5 DH270UCA knock-in mice immunized with 10.17DT (x-axis), was plotted against the enrichment of the same mutations in library clones selected by 10.17DT from C (y-axis). Data was fitted with a linear equation (R^2=0.625). Immunization enrichment was determined by calculating the ratio between the frequency of the observed mutations in the antibody repertoire of vaccinated animals analyzed by next generation sequencing, and the expected frequency of the mutations in the absence of immunogen selection predicted with ARMADiLLO (Wiehe et al., 2018). Immunization data is available only for the heavy chain sequences (Saunders et al., 2019).

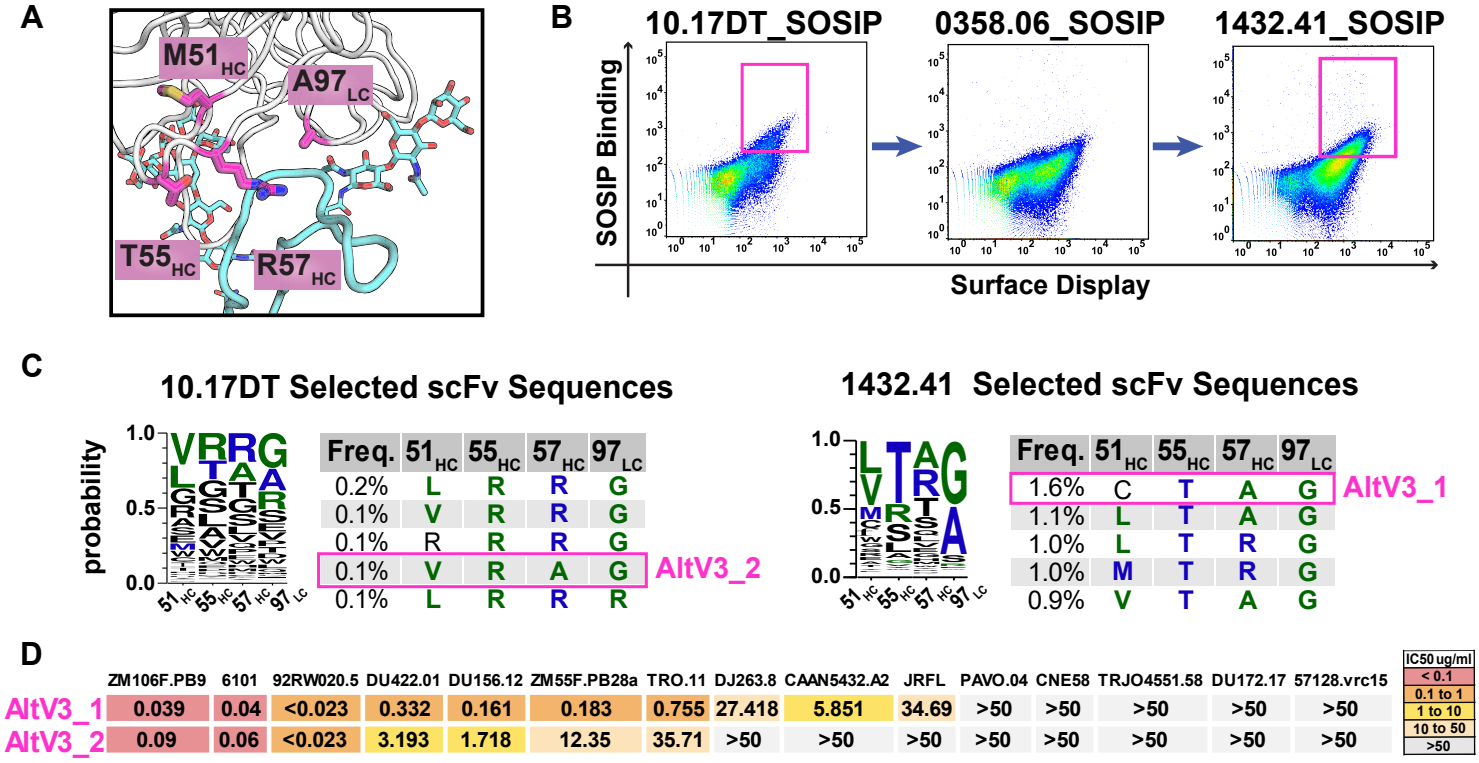

Figure 5. Identification of alternative, more probable, amino acids at the DH270min11 acquired mutation sites that contact the Env V3 loop. A. DH270min11 acquired mutations (*magenta, sticks*) that interact with the V3 loop (*cyan*, glycans shown in sticks) (PDBid:6cbp). **B.** FACS analysis of the scFv library that contains all possible amino acid combinations at the DH270min11 sites in **A**, for serial binding to three different SOSIPs. The sequence of the clones sorted in the displayed gates (*magenta*) was analyzed by PacBio. **C.** Sequence analysis of the clones selected in **B**. The native DH270.6 amino acid is shown in blue, while mutations more probable than the native DH270.6 amino acid at a given site are marked in green. Sequence tables show the frequency of the five most common DH270min11 variants selected by 10.17DT (*left*) and 1432.41 (*right*) SOSIP. **D.** Neutralization profile of two selected DH270min11 variants, AltV3_1 and AltV3_2, on a panel of 15 DH270.6 sensitive pseudoviruses.

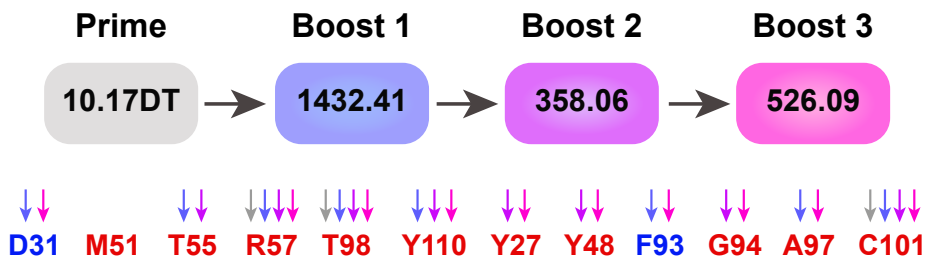

Figure 6. Vaccination regimen for the elicitation of DH270.6-like antibodies that contain the key functional mutations. Priming with the germline targeting immunogen 10.17DT will be followed by successive boosts with molecules identified in this study. Arrows point to the DH270min11 acquired mutations predicted to be selected by the immunogen depicted in the same color. Mutations are colored by probability (red=improbable; blue=probable).

A.

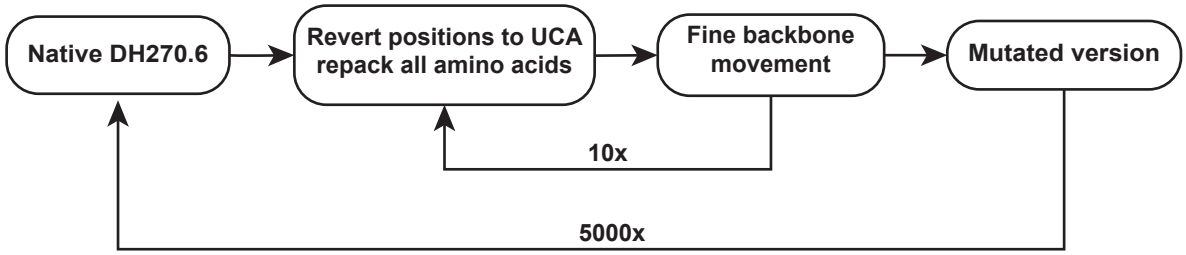

B.

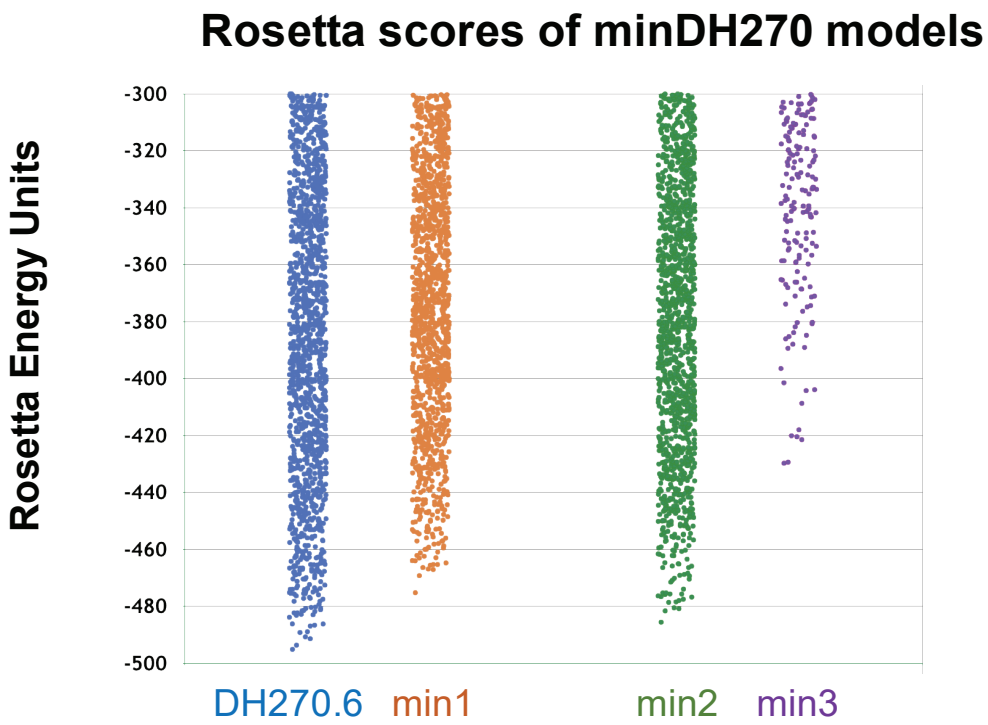

min1 UCA + binding interface + 2nd shell improbable muts

min2 UCA + binding interface + 2nd shell improbable + H/L chain interface muts

min3 UCA+ binding interface muts

Supplementary Figure 1. **Computational design of minimized DH270.6 antibodies**. **A.** Rosetta protocol to evaluate the effect of acquired mutations on antibody packing and stability. **B.** Rosetta energy landscapes of designed mins (5000 decoys) described in **A** and chosen for experimental characterization.

High Throughput Antibody Screen - Panel 38

Assay - Luc/TZM-bl
values represent IC50 in ug/ml

ug/mL	
<0.001	.100-1.00
.001-.01	1.00-10.0
.01-.100	>10.0

previous data *Bonsignori et.al 2017

Virus ID	Clade	DH270.min1	DH270.min11	DH270.min12		DH270	DH270_IA1	DH270_IA2	DH270_IA4
0260.v5.c36	A	0.351	0.433	1.37		2.32	0.295	2.17	>50
0330.v4.c3	A	>50	>50	>50		>50	>50	>50	>50
0439.v5.c1	A	>50	>50	>50		>50	>50	>50	>50
3365.v2.c20	A	>50	>50	>50		>50	>50	>50	>50
3415.v1.c1	A	>50	>50	>50		>50	>50	>50	>50
3718.v3.c11	A	>50	>50	>50		>50	>50	>50	>50
398-F1.F6.20	A	0.016	0.015	0.030		0.038	0.010	0.026	1.14
BB201.B42	A	>50	>50	>50		>50	>50	>50	>50
BB539.2B13	A	>50	>50	>50		>50	>50	>50	>50
BG505.W6M.C2	A	>50	>50	>50		>50	>50	>50	>50
BI369.9A	A	0.103	0.111	0.325		0.407	0.086	0.579	>50
BS208.B1	A	>50	>50	>50		>50	>50	>50	>50
KER2008.12	A	0.076	0.214	>50		14.6	0.080	>50	>50
KER2018.11	A	>50	>50	>50		>50	>50	>50	>50
KNH1209.18	A	0.021	0.025	0.026		0.085	0.032	0.082	2.74
MB201.A1	A	>50	>50	>50		>50	>50	>50	>50
MB539.2B7	A	>50	>50	>50		>50	>50	>50	>50
MI369.A5	A	0.129	0.196	0.146		0.501	0.221	0.620	>50
MS208.A1	A	>50	>50	>50		>50	>50	>50	>50
Q23.17	A	0.020	0.024	0.024		0.058	0.022	0.074	16.3
Q259.17	A	>50	>50	>50		>50	>50	>50	>50
Q769.d22	A	>50	>50	>50		>50	>50	>50	>50
Q769.h5	A	>50	>50	>50		>50	>50	>50	>50
Q842.d12	A	>50	>50	>50		>50	>50	>50	>50
QH209.14M.A2	A	>50	>50	>50		>50	>50	>50	>50
RW020.2	A	0.012	0.006	0.007		0.051	0.010	0.023	0.176
UG037.8	A	0.101	0.219	>50		1.53	0.317	>50	>50
246-F3.C10.2	AC	>50	>50	>50		>50	>50	>50	>50
3301.v1.c24	AC	0.080	0.115	5.53		0.587	0.109	>50	>50
3589.v1.c4	AC	>50	>50	>50		>50	>50	>50	>50
6540.v4.c1	AC	>50	>50	>50		>50	>50	>50	>50
6545.v4.c1	AC	>50	>50	>50		>50	>50	>50	>50
0815.v3.c3	ACD	0.150	0.139	0.136		0.635	0.127	0.380	3.50
6095.v1.c10	ACD	>50	>50	>50		>50	>50	>50	>50
3468.v1.c12	AD	>50	>50	>50		>50	>50	>50	>50
Q168.a2	AD	>50	>50	>50		>50	>50	>50	>50
Q461.e2	AD	>50	>50	>50		>50	>50	>50	>50
620345.c1	AE	>50	>50	>50		>50	>50	>50	>50
BJOX009000.02.4	AE	>50	>50	>50		>50	>50	>50	>50
BJOX010000.06.2	AE	>50	>50	>50		>50	>50	>50	>50
BJOX025000.01.1	AE	>50	>50	>50		>50	>50	>50	>50
BJOX028000.10.3	AE	>50	>50	>50		>50	>50	>50	>50
C1080.c3	AE	>50	>50	>50		>50	>50	>50	>50
C2101.c1	AE	>50	>50	>50		>50	>50	>50	>50
C3347.c11	AE	>50	>50	>50		>50	>50	>50	>50
C4118.09	AE	>50	>50	>50		>50	>50	>50	>50
CM244.ec1	AE	>50	>50	>50		>50	>50	>50	>50

CNE3	AE	>50	>50	>50		>50	>50	>50	>50
CNE5	AE	>50	>50	>50		>50	>50	>50	>50
CNE55	AE	>50	>50	>50		>50	>50	>50	>50
CNE56	AE	>50	>50	>50		>50	>50	>50	>50
CNE59	AE	>50	>50	>50		>50	>50	>50	>50
CNE8	AE	>50	>50	>50		>50	>50	>50	>50
M02138	AE	>50	>50	>50		>50	>50	>50	>50
R1166.c1	AE	>50	>50	>50		>50	>50	>50	>50
R2184.c4	AE	>50	>50	>50		>50	>50	>50	>50
R3265.c6	AE	>50	>50	>50		>50	>50	>50	>50
TH023.6	AE	>50	>50	>50		>50	>50	>50	>50
TH966.8	AE	>50	>50	>50		>50	>50	>50	>50
TH976.17	AE	>50	>50	>50		>50	>50	>50	>50
235-47	AG	0.185	0.240	11.5		3.11	0.118	>50	>50
242-14	AG	>50	>50	>50		>50	>50	>50	>50
263-8	AG	1.12	5.06	>50		>50	9.03	>50	>50
269-12	AG	0.089	0.139	>50		2.74	0.096	>50	>50
271-11	AG	>50	>50	>50		>50	>50	>50	>50
928-28	AG	23.0	21.7	>50		>50	8.00	>50	>50
DJ263.8	AG	0.083	0.102	1.56		0.201	0.072	0.598	>50
T250-4	AG	>50	>50	>50		>50	>50	>50	>50
T251-18	AG	>50	>50	>50		>50	>50	>50	>50
T253-11	AG	>50	>50	>50		>50	>50	>50	>50
T255-34	AG	>50	>50	>50		>50	>50	>50	>50
T257-31	AG	>50	>50	>50		>50	>50	>50	>50
T266-60	AG	0.952	2.74	>50		6.21	0.787	>50	>50
T278-50	AG	>50	>50	>50		>50	>50	>50	>50
T280-5	AG	0.015	0.018	0.020		0.044	0.013	0.067	39.5
T33-7	AG	>50	>50	>50		>50	>50	>50	>50
3988.25	B	0.017	0.020	1.07		0.090	0.021	0.463	>50
5768.04	B	0.314	0.927	>50		>50	0.079	>50	>50
6101.10	B	0.035	0.039	0.023		0.124	0.027	0.116	1.45
6535.3	B	0.025	0.029	0.022		0.102	0.023	0.069	0.432
7165.18	B	0.056	0.068	0.710		0.281	0.043	1.11	>50
45_01dG5	B	0.037	0.057	0.063		0.099	0.074	0.177	16.3
89.6.DG	B	0.039	0.044	44.7		0.267	0.056	>50	>50
AC10.29	B	0.019	0.022	>50		1.18	0.012	>50	>50
ADA.DG	B	0.060	0.076	0.892		0.463	0.047	1.21	>50
Bal.01	B	0.054	0.055	0.331		0.176	0.032	0.300	>50
BaL.26	B	0.034	0.039	0.105		0.221	0.027	0.226	>50
BG1168.01	B	>50	>50	>50		>50	>50	>50	>50
BL01.DG	B	20.0	>50	>50		>50	>50	>50	>50
BR07.DG	B	>50	>50	>50		>50	>50	>50	>50
BX08.16	B	0.015	0.019	0.030		0.074	0.006	0.053	9.78
CAAN.A2	B	0.018	0.035	2.53		0.088	0.030	8.69	>50
CNE10	B	>50	>50	>50		>50	>50	>50	>50
CNE12	B	0.052	0.057	0.051		0.128	0.052	0.111	13.1
CNE14	B	0.022	0.025	0.023		0.066	0.019	0.049	0.761
CNE4	B	>50	>50	>50		>50	>50	>50	>50
CNE57	B	0.056	0.059	0.530		0.135	0.068	1.15	>50
HO86.8	B	>50	>50	>50		>50	>50	>50	>50
HT593.1	B	>50	>50	>50		>50	>50	>50	>50
HXB2.DG	B	>50	>50	>50		>50	>50	>50	>50
JRCSF.JB	B	0.049	0.077	47.7		1.17	0.069	>50	>50
JRFL.JB	B	0.028	0.025	0.182		0.075	0.018	0.396	>50
MN.3	B	>50	>50	>50		>50	>50	>50	>50
PVO.04	B	0.082	0.103	>50		0.447	0.146	>50	>50

QH0515.01	B	4.94	21.2	>50		>50	45.1	>50	>50
QH0692.42	B	0.216	0.288	>50		3.96	0.437	>50	>50
REJO.67	B	>50	>50	>50		>50	>50	>50	>50
RHPA.7	B	0.048	0.055	22.5		0.285	0.092	40.6	>50
SC422.8	B	0.087	0.085	49.3		0.646	0.091	>50	>50
SF162.LS	B	0.012	0.016	0.031		0.036	0.006	0.026	1.53
SS1196.01	B	0.036	0.040	0.645		0.080	0.046	0.633	>50
THRO.18	B	>50	>50	>50		>50	>50	>50	>50
TRJO.58	B	0.241	0.440	>50		>50	0.099	>50	>50
TRO.11	B	0.049	0.064	0.094		0.189	0.039	0.091	25.6
WITO.33	B	>50	>50	>50		>50	>50	>50	>50
X2278.C2.B6	B	0.047	0.069	>50		0.855	0.030	>50	>50
YU2.DG	B	0.111	0.147	0.857		0.634	0.070	0.742	>50
BJOX002000.03.2	BC	0.019	0.021	0.026		0.096	0.015	0.181	>50
CH038.12	BC	0.034	0.038	>50		0.217	0.033	>50	>50
CH070.1	BC	0.119	0.126	1.25		0.621	0.058	22.1	>50
CH117.4	BC	>50	>50	>50		>50	>50	>50	>50
CH119.10	BC	0.058	0.056	0.064		0.235	0.028	0.159	>50
CH181.12	BC	0.086	0.145	44.2		0.773	0.349	>50	>50
CNE15	BC	>50	>50	>50		>50	>50	>50	>50
CNE19	BC	0.048	0.140	>50		>50	0.104	>50	>50
CNE20	BC	>50	>50	>50		>50	>50	>50	>50
CNE21	BC	0.038	0.050	40.4		0.535	0.049	>50	>50
CNE40	BC	>50	>50	>50		>50	>50	>50	>50
CNE7	BC	>50	>50	>50		>50	>50	>50	>50
286.36	C	0.038	0.057	0.120		0.119	0.041	0.085	18.6
288.38	C	0.028	0.028	0.057		0.148	0.049	0.104	7.76
0013095-2.11	C	>50	>50	>50		>50	>50	>50	>50
001428-2.42	C	>50	>50	>50		>50	>50	>50	>50
0077.v1.c16	C	>50	>50	>50		>50	>50	>50	>50
00836-2.5	C	>50	>50	>50		>50	>50	>50	>50
0921.v2.c14	C	>50	>50	>50		>50	>50	>50	>50
16055-2.3	C	>50	>50	>50		>50	>50	>50	>50
16845-2.22	C	2.20	1.80	>50		>50	2.17	>50	>50
16936-2.21	C	0.051	0.066	0.404		0.725	0.073	32.1	>50
25710-2.43	C	0.112	0.153	32.4		2.07	0.170	>50	>50
25711-2.4	C	0.018	0.019	0.571		0.200	0.023	>50	>50
25925-2.22	C	8.27	7.12	>50		>50	11.2	>50	>50
26191-2.48	C	>50	>50	>50		>50	>50	>50	>50
3168.v4.c10	C	0.218	0.167	28.8		0.856	0.396	>50	>50
3637.v5.c3	C	>50	>50	>50		>50	>50	>50	>50
3873.v1.c24	C	0.056	0.052	8.95		0.374	0.091	>50	>50
426c	C	0.981	2.09	>50		>50	1.97	>50	>50
6322.v4.c1	C	>50	>50	>50		>50	>50	>50	>50
6471.v1.c16	C	6.82	5.04	>50		>50	1.26	>50	>50
6631.v3.c10	C	>50	>50	>50		>50	>50	>50	>50
6644.v2.c33	C	0.025	0.031	0.174		0.128	0.031	0.148	>50
6785.v5.c14	C	0.050	0.054	0.174		0.247	0.033	0.462	>50
6838.v1.c35	C	>50	>50	>50		>50	>50	>50	>50
96ZM651.02	C	0.022	0.025	5.65		0.660	0.016	18.1	>50
BR025.9	C	0.011	0.013	0.016		0.060	0.011	0.032	0.500
CAP210.E8	C	>50	>50	>50		>50	>50	>50	>50
CAP244.D3	C	>50	>50	>50		>50	14.4	>50	>50
CAP256.206.C9	C	0.053	0.049	0.043		0.128	0.040	0.125	>50
CAP45.G3	C	>50	>50	>50		>50	>50	>50	>50
Ce1176.A3	C	0.066	0.075	0.115		0.294	0.076	0.204	>50
CE703010217.B6	C	0.033	0.041	0.144		0.457	0.023	>50	>50

CNE30	C	1.02	0.765	4.54		3.02	0.801	9.12	>50
CNE31	C	>50	>50	>50		>50	>50	>50	>50
CNE53	C	0.103	0.102	0.100		0.406	0.107	0.513	>50
CNE58	C	0.208	0.270	43.7		2.20	0.284	>50	>50
DU123.06	C	0.102	0.126	0.193		0.531	0.112	0.591	>50
DU151.02	C	>50	>50	>50		>50	>50	>50	>50
DU156.12	C	0.077	0.088	0.087		0.234	0.055	0.323	>50
DU172.17	C	1.29	1.81	>50		13.8	0.428	>50	>50
DU422.01	C	0.144	0.232	0.211		0.554	0.147	28.0	>50
MW965.26	C	0.027	0.026	>50		0.135	0.036	>50	>50
SO18.18	C	0.023	0.030	0.141		0.073	0.025	0.374	>50
TV1.29	C	1.06	0.828	16.9		8.94	0.742	15.8	>50
TZA125.17	C	>50	>50	>50		>50	>50	>50	>50
TZBD.02	C	0.053	0.060	0.212		1.82	0.078	>50	>50
ZA012.29	C	0.040	0.054	2.71		9.33	0.055	>50	>50
ZM106.9	C	0.034	0.044	0.054		0.127	0.057	0.381	>50
ZM109.4	C	>50	>50	>50		>50	>50	>50	>50
ZM135.10a	C	0.110	0.240	>50		2.12	0.142	>50	>50
ZM176.66	C	2.65	2.77	>50		>50	14.7	>50	>50
ZM197.7	C	>50	>50	>50		>50	>50	>50	>50
ZM214.15	C	1.58	2.26	>50		46.9	1.32	>50	>50
ZM215.8	C	1.76	1.52	>50		5.13	0.547	>50	>50
ZM233.6	C	>50	>50	>50		>50	>50	>50	>50
ZM249.1	C	>50	>50	>50		>50	>50	>50	>50
ZM53.12	C	>50	>50	>50		>50	>50	>50	>50
ZM55.28a	C	0.030	0.044	0.057		0.145	0.036	0.072	43.7
3326.v4.c3	CD	>50	>50	>50		>50	>50	>50	>50
3337.v2.c6	CD	31.3	35.4	>50		34.0	>50	>50	>50
3817.v2.c59	CD	0.221	0.327	>50		0.736	0.222	>50	>50
191821.E6.1	D	>50	>50	>50		>50	>50	>50	>50
231965.c01	D	>50	>50	>50		>50	>50	>50	>50
247-23	D	>50	>50	>50		>50	>50	>50	>50
3016.v5.c45	D	>50	>50	>50		>50	>50	>50	>50
57128.vrc15	D	26.6	25.6	>50		17.4	>50	>50	>50
6405.v4.c34	D	>50	>50	>50		>50	>50	>50	>50
A03349M1.vrc4a	D	>50	>50	>50		>50	>50	>50	>50
A07412M1.vrc12	D	>50	>50	>50		>50	>50	>50	>50
NKU3006.ec1	D	>50	>50	>50		>50	>50	>50	>50
UG021.16	D	>50	>50	>50		>50	>50	>50	>50
UG024.2	D	>50	>50	>50		>50	>50	>50	>50
P0402.c2.11	G	3.83	3.53	>50		14.8	5.20	>50	>50
P1981.C5.3	G	0.013	0.013	0.015		0.047	0.011	0.031	11.6
X1193.c1	G	1.07	1.70	>50		31.3	0.372	>50	>50
X1254.c3	G	0.067	0.078	2.08		0.259	0.082	17.3	>50
X1632.S2.B10	G	>50	>50	>50		>50	>50	>50	>50
X2088.c9	G	0.020	0.029	0.065		0.158	0.027	6.68	>50
X2131.C1.B5	G	0.169	0.214	>50		0.972	0.079	>50	>50
SIVmac251.30.SG3	NA	>50	>50	>50		>50	>50	>50	>50
SVA.MLV	NA	>50	>50	>50		>50	>50	>50	>50

	DH270.min1	DH270.min11	DH270.min12	DH270	DH270_IA1	DH270_IA2	DH270_IA4
# Viruses	208	208	208	208	208	208	208
Total VS Neutralized IC50 <50ug/ml	100	99	68	88	98	53	19

IC50 <10ug/ml	96	95	57	81	94	46	11
IC50 <1.0ug/ml	83	83	46	65	87	39	4
IC50 <0.1ug/ml	61	54	23	17	63	14	0
IC50 <0.01ug/ml	0	1	1	0	2	0	0
% VS Neutralized							
IC50 <50ug/ml	48	48	33	42	47	25	9
IC50 <10ug/ml	46	46	27	39	45	22	5
IC50 <1.0ug/ml	40	40	22	31	42	19	2
IC50 <0.1ug/ml	29	26	11	8	30	7	0
IC50 <0.01ug/ml	0	0	0	0	1	0	0
Median IC50	0.059	0.076	0.188	0.390	0.073	0.374	7.76
Geometric Mean	0.113	0.135	0.408	0.482	0.103	0.449	4.41

Note: Median and Geometric Mean titers are calculated only for samples with IC50 <50ug/ml

High Throughput Antibody Screen - Panel 38

Assay - Luc/TZM-bl
values represent IC80 in ug/ml

ug/mL	
<0.001	.100-1.00
.001-.01	1.00-10.0
.01-.100	>10.0

IC80

previous data *Bonsignori et.al 2017

Virus ID	Clade	DH270. min1	DH270. min11	DH270. min12	DH270	DH270_IA 1	DH270_IA 2	DH270_IA 4
0260.v5.c36	A	0.699	0.999	3.54	5.38	0.995	8.09	>50
0330.v4.c3	A	>50	>50	>50	>50	>50	>50	>50
0439.v5.c1	A	>50	>50	>50	>50	>50	>50	>50
3365.v2.c20	A	>50	>50	>50	>50	>50	>50	>50
3415.v1.c1	A	>50	>50	>50	>50	>50	>50	>50
3718.v3.c11	A	>50	>50	>50	>50	>50	>50	>50
398-F1.F6.20	A	0.040	0.038	0.064	0.101	0.033	0.086	7.39
BB201.B42	A	>50	>50	>50	>50	>50	>50	>50
BB539.2B13	A	>50	>50	>50	>50	>50	>50	>50
BG505.W6M.C2	A	>50	>50	>50	>50	>50	>50	>50
BI369.9A	A	0.230	0.309	1.48	1.01	0.299	3.64	>50
BS208.B1	A	>50	>50	>50	>50	>50	>50	>50
KER2008.12	A	0.585	1.89	>50	>50	0.654	>50	>50
KER2018.11	A	>50	>50	>50	>50	>50	>50	>50
KNH1209.18	A	0.050	0.067	0.081	0.205	0.077	0.177	11.3
MB201.A1	A	>50	>50	>50	>50	>50	>50	>50
MB539.2B7	A	>50	>50	>50	>50	>50	>50	>50
MI369.A5	A	0.316	0.408	0.459	1.32	0.554	1.41	>50
MS208.A1	A	>50	>50	>50	>50	>50	>50	>50
Q23.17	A	0.046	0.066	0.075	0.138	0.061	0.160	>50
Q259.17	A	>50	>50	>50	>50	>50	>50	>50
Q769.d22	A	>50	>50	>50	>50	>50	>50	>50
Q769.h5	A	>50	>50	>50	>50	>50	>50	>50
Q842.d12	A	>50	>50	>50	>50	>50	>50	>50
QH209.14M.A2	A	>50	>50	>50	>50	>50	>50	>50
RW020.2	A	0.026	0.027	0.025	0.116	0.035	0.062	0.910
UG037.8	A	0.353	1.11	>50	7.61	2.13	>50	>50
246-F3.C10.2	AC	>50	>50	>50	>50	>50	>50	>50
3301.v1.c24	AC	0.213	0.297	>50	1.50	0.362	>50	>50
3589.v1.c4	AC	>50	>50	>50	>50	>50	>50	>50
6540.v4.c1	AC	>50	>50	>50	>50	>50	>50	>50
6545.v4.c1	AC	>50	>50	>50	>50	>50	>50	>50
0815.v3.c3	ACD	0.375	0.358	0.441	1.64	0.571	1.03	24.1
6095.v1.c10	ACD	>50	>50	>50	>50	>50	>50	>50
3468.v1.c12	AD	>50	>50	>50	>50	>50	>50	>50
Q168.a2	AD	>50	>50	>50	>50	>50	>50	>50
Q461.e2	AD	>50	>50	>50	>50	>50	>50	>50
620345.c1	AE	>50	>50	>50	>50	>50	>50	>50
BJOX009000.02.4	AE	>50	>50	>50	>50	>50	>50	>50
BJOX010000.06.2	AE	>50	>50	>50	>50	>50	>50	>50
BJOX025000.01.1	AE	>50	>50	>50	>50	>50	>50	>50
BJOX028000.10.3	AE	>50	>50	>50	>50	>50	>50	>50
C1080.c3	AE	>50	>50	>50	>50	>50	>50	>50
C2101.c1	AE	>50	>50	>50	>50	>50	>50	>50
C3347.c11	AE	>50	>50	>50	>50	>50	>50	>50
C4118.09	AE	>50	>50	>50	>50	>50	>50	>50
CM244.ec1	AE	>50	>50	>50	>50	>50	>50	>50
CNE3	AE	>50	>50	>50	>50	>50	>50	>50

CNE5	AE	>50	>50	>50	>50	>50	>50	>50
CNE55	AE	>50	>50	>50	>50	>50	>50	>50
CNE56	AE	>50	>50	>50	>50	>50	>50	>50
CNE59	AE	>50	>50	>50	>50	>50	>50	>50
CNE8	AE	>50	>50	>50	>50	>50	>50	>50
M02138	AE	>50	>50	>50	>50	>50	>50	>50
R1166.c1	AE	>50	>50	>50	>50	>50	>50	>50
R2184.c4	AE	>50	>50	>50	>50	>50	>50	>50
R3265.c6	AE	>50	>50	>50	>50	>50	>50	>50
TH023.6	AE	>50	>50	>50	>50	>50	>50	>50
TH966.8	AE	>50	>50	>50	>50	>50	>50	>50
TH976.17	AE	>50	>50	>50	>50	>50	>50	>50
235-47	AG	0.490	0.492	>50	12.1	0.564	>50	>50
242-14	AG	>50	>50	>50	>50	>50	>50	>50
263-8	AG	10.8	>50	>50	>50	>50	>50	>50
269-12	AG	0.611	0.987	>50	9.15	1.56	>50	>50
271-11	AG	>50	>50	>50	>50	>50	>50	>50
928-28	AG	>50	>50	>50	>50	>50	>50	>50
DJ263.8	AG	0.233	0.315	>50	0.865	0.184	3.32	>50
T250-4	AG	>50	>50	>50	>50	>50	>50	>50
T251-18	AG	>50	>50	>50	>50	>50	>50	>50
T253-11	AG	>50	>50	>50	>50	>50	>50	>50
T255-34	AG	>50	>50	>50	>50	>50	>50	>50
T257-31	AG	>50	>50	>50	>50	>50	>50	>50
T266-60	AG	7.59	24.1	>50	30.9	19.0	>50	>50
T278-50	AG	>50	>50	>50	>50	>50	>50	>50
T280-5	AG	0.039	0.042	0.053	0.169	0.048	0.244	>50
T33-7	AG	>50	>50	>50	>50	>50	>50	>50
3988.25	B	0.047	0.053	7.43	0.184	0.056	2.81	>50
5768.04	B	5.41	21.4	>50	>50	0.799	>50	>50
6101.10	B	0.093	0.080	0.076	0.327	0.083	0.287	8.57
6535.3	B	0.067	0.074	0.067	0.276	0.066	0.177	1.61
7165.18	B	0.138	0.188	9.08	0.815	0.140	18.6	>50
45_01dG5	B	0.093	0.152	0.185	0.301	0.241	0.568	>50
89.6.DG	B	0.120	0.151	>50	0.628	0.265	>50	>50
AC10.29	B	0.049	0.056	>50	4.47	0.057	>50	>50
ADA.DG	B	0.177	0.244	>50	1.97	0.221	>50	>50
Bal.01	B	0.156	0.154	>50	0.636	0.120	>50	>50
BaL.26	B	0.097	0.133	3.21	0.541	0.112	0.516	>50
BG1168.01	B	>50	>50	>50	>50	>50	>50	>50
BL01.DG	B	>50	>50	>50	>50	>50	>50	>50
BR07.DG	B	>50	>50	>50	>50	>50	>50	>50
BX08.16	B	0.042	0.048	0.091	0.198	0.047	0.156	>50
CAAN.A2	B	0.052	0.090	>50	0.267	0.092	>50	>50
CNE10	B	>50	>50	>50	>50	>50	>50	>50
CNE12	B	0.085	0.090	0.162	0.325	0.133	0.292	>50
CNE14	B	0.050	0.063	0.071	0.153	0.065	0.121	6.23
CNE4	B	>50	>50	>50	>50	>50	>50	>50
CNE57	B	0.120	0.130	3.87	0.291	0.193	6.31	>50
HO86.8	B	>50	>50	>50	>50	>50	>50	>50
HT593.1	B	>50	>50	>50	>50	>50	>50	>50
HXB2.DG	B	>50	>50	>50	>50	>50	>50	>50
JRCSF.JB	B	0.159	0.306	>50	4.55	0.307	>50	>50
JRFL.JB	B	0.064	0.063	1.25	0.202	0.059	3.61	>50
MN.3	B	>50	>50	>50	>50	>50	>50	>50
PVO.04	B	0.232	0.303	>50	1.39	0.633	>50	>50
QH0515.01	B	>50	>50	>50	>50	>50	>50	>50

QH0692.42	B	0.737	1.60	>50	24.1	2.27	>50	>50
REJO.67	B	>50	>50	>50	>50	>50	>50	>50
RHPA.7	B	0.138	0.235	>50	1.20	0.260	>50	>50
SC422.8	B	0.198	0.223	>50	1.82	0.337	>50	>50
SF162.LS	B	0.025	0.037	0.096	0.096	0.044	0.068	>50
SS1196.01	B	0.078	0.089	5.91	0.214	0.106	5.39	>50
THRO.18	B	>50	>50	>50	>50	>50	>50	>50
TRJO.58	B	0.667	1.73	>50	>50	0.470	>50	>50
TRO.11	B	0.126	0.148	0.309	0.510	0.120	0.291	>50
WITO.33	B	>50	>50	>50	>50	>50	>50	>50
X2278.C2.B6	B	0.120	0.187	>50	4.58	0.137	>50	>50
YU2.DG	B	0.321	0.387	25.4	1.81	0.195	3.83	>50
BJOX002000.03.2	BC	0.048	0.059	0.074	0.236	0.048	1.05	>50
CH038.12	BC	0.109	0.113	>50	0.674	0.123	>50	>50
CH070.1	BC	0.291	0.351	11.3	1.70	0.237	>50	>50
CH117.4	BC	>50	>50	>50	>50	>50	>50	>50
CH119.10	BC	0.091	0.140	0.185	0.412	0.084	0.381	>50
CH181.12	BC	0.230	0.376	>50	2.52	1.14	>50	>50
CNE15	BC	>50	>50	>50	>50	>50	>50	>50
CNE19	BC	>50	>50	>50	>50	>50	>50	>50
CNE20	BC	>50	>50	>50	>50	>50	>50	>50
CNE21	BC	0.112	0.138	>50	1.61	0.153	>50	>50
CNE40	BC	>50	>50	>50	>50	>50	>50	>50
CNE7	BC	>50	>50	>50	>50	>50	>50	>50
286.36	C	0.106	0.147	0.328	0.342	0.088	0.200	>50
288.38	C	0.062	0.090	0.166	0.390	0.128	0.299	44.5
0013095-2.11	C	>50	>50	>50	>50	>50	>50	>50
001428-2.42	C	>50	>50	>50	>50	>50	>50	>50
0077.v1.c16	C	>50	>50	>50	>50	>50	>50	>50
00836-2.5	C	>50	>50	>50	>50	>50	>50	>50
0921.v2.c14	C	>50	>50	>50	>50	>50	>50	>50
16055-2.3	C	>50	>50	>50	>50	>50	>50	>50
16845-2.22	C	8.38	10.5	>50	>50	9.28	>50	>50
16936-2.21	C	0.136	0.243	2.19	2.05	0.234	>50	>50
25710-2.43	C	0.301	0.383	>50	8.80	0.450	>50	>50
25711-2.4	C	0.042	0.051	3.36	1.50	0.051	>50	>50
25925-2.22	C	>50	>50	>50	>50	>50	>50	>50
26191-2.48	C	>50	>50	>50	>50	>50	>50	>50
3168.v4.c10	C	0.654	0.839	>50	4.14	1.38	>50	>50
3637.v5.c3	C	>50	>50	>50	>50	>50	>50	>50
3873.v1.c24	C	0.125	0.159	>50	0.976	0.258	>50	>50
426c	C	24.2	>50	>50	>50	>50	>50	>50
6322.v4.c1	C	>50	>50	>50	>50	>50	>50	>50
6471.v1.c16	C	>50	>50	>50	>50	10.1	>50	>50
6631.v3.c10	C	>50	>50	>50	>50	>50	>50	>50
6644.v2.c33	C	0.095	0.106	>50	0.328	0.122	0.660	>50
6785.v5.c14	C	0.118	0.140	1.09	0.525	0.115	1.66	>50
6838.v1.c35	C	>50	>50	>50	>50	>50	>50	>50
96ZM651.02	C	0.102	0.348	>50	>50	0.429	>50	>50
BR025.9	C	0.032	0.045	0.042	0.127	0.039	0.078	1.97
CAP210.E8	C	>50	>50	>50	>50	>50	>50	>50
CAP244.D3	C	>50	>50	>50	>50	>50	>50	>50
CAP256.206.C9	C	0.114	0.129	0.119	0.325	0.105	0.328	>50
CAP45.G3	C	>50	>50	>50	>50	>50	>50	>50
Ce1176.A3	C	0.188	0.190	0.349	0.755	0.238	0.499	>50
CE703010217.B6	C	0.087	0.110	0.660	1.81	0.076	>50	>50
CNE30	C	2.03	2.30	16.6	6.49	2.18	40.6	>50

CNE31	C	>50	>50	>50	>50	>50	>50	>50
CNE53	C	0.297	0.323	0.330	1.14	0.306	1.25	>50
CNE58	C	0.659	0.650	>50	10.3	0.865	>50	>50
DU123.06	C	0.280	0.377	1.15	1.72	0.362	4.46	>50
DU151.02	C	>50	>50	>50	>50	>50	>50	>50
DU156.12	C	0.155	0.216	0.264	0.710	0.159	1.53	>50
DU172.17	C	12.2	23.3	>50	>50	5.12	>50	>50
DU422.01	C	0.380	0.481	0.539	1.30	0.391	>50	>50
MW965.26	C	0.119	0.104	>50	0.773	0.121	>50	>50
SO18.18	C	0.059	0.070	0.695	0.167	0.081	2.32	>50
TV1.29	C	3.86	3.15	>50	26.1	2.96	>50	>50
TZA125.17	C	>50	>50	>50	>50	>50	>50	>50
TZBD.02	C	0.125	0.186	2.13	10.4	0.256	>50	>50
ZA012.29	C	0.107	0.158	>50	>50	0.187	>50	>50
ZM106.9	C	0.088	0.122	0.117	0.316	0.136	2.13	>50
ZM109.4	C	>50	>50	>50	>50	>50	>50	>50
ZM135.10a	C	0.391	1.02	>50	18.7	0.559	>50	>50
ZM176.66	C	15.6	21.6	>50	>50	>50	>50	>50
ZM197.7	C	>50	>50	>50	>50	>50	>50	>50
ZM214.15	C	4.38	9.36	>50	>50	15.0	>50	>50
ZM215.8	C	25.7	15.0	>50	31.1	8.29	>50	>50
ZM233.6	C	>50	>50	>50	>50	>50	>50	>50
ZM249.1	C	>50	>50	>50	>50	>50	>50	>50
ZM53.12	C	>50	>50	>50	>50	>50	>50	>50
ZM55.28a	C	0.072	0.118	0.147	0.329	0.113	0.206	>50
3326.v4.c3	CD	>50	>50	>50	>50	>50	>50	>50
3337.v2.c6	CD	>50	>50	>50	>50	>50	>50	>50
3817.v2.c59	CD	0.856	1.39	>50	2.76	1.02	>50	>50
191821.E6.1	D	>50	>50	>50	>50	>50	>50	>50
231965.c01	D	>50	>50	>50	>50	>50	>50	>50
247-23	D	>50	>50	>50	>50	>50	>50	>50
3016.v5.c45	D	>50	>50	>50	>50	>50	>50	>50
57128.vrc15	D	>50	>50	>50	>50	>50	>50	>50
6405.v4.c34	D	>50	>50	>50	>50	>50	>50	>50
A03349M1.vrc4a	D	>50	>50	>50	>50	>50	>50	>50
A07412M1.vrc12	D	>50	>50	>50	>50	>50	>50	>50
NKU3006.ec1	D	>50	>50	>50	>50	>50	>50	>50
UG021.16	D	>50	>50	>50	>50	>50	>50	>50
UG024.2	D	>50	>50	>50	>50	>50	>50	>50
P0402.c2.11	G	49.5	45.4	>50	>50	>50	>50	>50
P1981.C5.3	G	0.029	0.031	0.058	0.108	0.028	0.125	>50
X1193.c1	G	5.39	8.05	>50	>50	1.90	>50	>50
X1254.c3	G	0.143	0.183	22.9	0.727	0.157	>50	>50
X1632.S2.B10	G	>50	>50	>50	>50	>50	>50	>50
X2088.c9	G	0.064	0.095	0.304	0.406	0.084	>50	>50
X2131.C1.B5	G	0.506	0.435	>50	5.13	0.416	>50	>50
SIVmac251.30.SG3	NA	>50	>50	>50	>50	>50	>50	>50
SVA.MLV	NA	>50	>50	>50	>50	>50	>50	>50

	DH270.min1	DH270.min11	DH270.min12	DH270	DH270_IA1	DH270_IA2	DH270_IA4
# Viruses	208	208	208	208	208	208	208
Total VS Neutralized							
IC80 <50ug/ml	92	90	48	79	89	42	9
IC80 <10ug/ml	86	83	44	71	86	40	6

IC80 <1.0ug/ml	79	73	31	42	74	23	1
IC80 <0.1ug/ml	30	23	13	1	23	4	0
IC80 <0.01ug/ml	0	0	0	0	0	0	0
% VS Neutralized							
IC80 <50ug/ml	44	43	23	38	43	20	4
IC80 <10ug/ml	41	40	21	34	41	19	3
IC80 <1.0ug/ml	38	35	15	20	36	11	0
IC80 <0.1ug/ml	14	11	6	0	11	2	0
IC80 <0.01ug/ml	0	0	0	0	0	0	0
Median IC80	0.138	0.188	0.329	0.815	0.195	0.542	7.39
Geometric Mean	0.246	0.303	0.493	1.02	0.267	0.739	6.21

Note: Median and Geometric Mean titers are calculated only for samples with IC50 <50ug/ml

Supplementary Figure 2. Neutralization profile of minimized DH270 variants on global panel. Values indicated calculated IC50 and IC80 of minDH270 against the individual viruses in the panel. DH270.6 neutralized 114 viruses from this panel with a mean IC50 of 0.136 ug/ml. DH270min1 neutralized 100 viruses (mean IC50=0.113 ug/ml), DH270min11 neutralized 99 viruses (mean IC50=0.135 ug/ml) and DH270min12 neutralized 68 viruses (mean IC50=0.408 ug/ml).

Fold binding decrease of DH270.min1 single residue reversion to UCA

	LogAUC DH270.6	HC.D31G	HC.M51I	HC.T55S	HC.R57G	HC.T98R	HC.Y110G	LC.Y27S	LC.Y48L	LC.F93Y	LC.G94A	LC.A97S	LC.C101F
10.17 [CH0848d0949.10.17D11gp120/293F/Mon]	13.175	1.0	1.0	1.0	1.1	1.2	1.3	1.1	1.1	1.0	1.0	1.0	1.0
1432.41 [CH848.3.d1432.5.41D11gp120/293F/Mon]	12.831	1.0	1.0	1.0	1.2	17.9	21.7	1.4	3.1	1.4	1.2	1.3	1.1
358.06 [CH848.3.d0358.80.06D11gp120]	10.718	1.2	1.4	1.2	3.1	NB	NB	2.6	53.9	3.2	1.7	1.6	1.4
526.02 [CH848.3.d0526.25.02D11gp120/293F]	7.015	1.5	1.2	1.3	8.5	NB	NB	13.5	NB	26.4	3.2	2.6	2.2
836.31 [CH0848d0836.10.31D11gp120/293F]	9.845	1.2	1.0	1.1	2.2	9.4	29.7	2.2	4.3	2.7	1.4	1.9	1.3
526.09 [CH848.3.d0526.25.09D11gp120/293F]	8.924	1.3	1.3	1.2	4.1	NB	NB	6.5	NB	11.0	2.4	2.4	1.7
CH848.3.d1120.10.41D11gp120/293F/PEI	13.274	1.0	1.0	1.0	1.0	1.1	1.2	1.1	1.1	1.0	1.0	1.0	1.0
CH848.3.d0864.7.26D11gp120	12.808	1.0	1.0	1.1	1.2	2.2	3.3	1.2	1.7	1.2	1.1	1.2	1.1
CH848.3d0808.15.25D11gp120	12.515	1.1	1.0	1.1	1.9	17.7	100.1	1.6	3.7	1.7	1.2	1.4	1.1
CH0848d0808.15.27D11gp120/293F	12.409	1.0	1.0	1.0	1.3	2.7	3.3	1.3	1.9	1.3	1.1	1.2	1.1
CH848.3.d1120.10.32D11gp120/293F/PEI	12.397	1.0	1.0	1.0	1.1	1.8	1.9	1.2	1.5	1.1	1.0	1.1	1.0
CH848.3.d0135.27.06D11gp120	12.091	1.1	1.5	1.1	2.1	NB	19.6	1.6	16.1	1.6	1.5	1.4	1.3
CH0848d0808.15.15D11gp120/293F	12.04	1.1	1.1	1.1	1.5	3.2	3.3	1.5	2.3	1.5	1.2	1.2	1.1
CH0848d1432.5.48D11gp120/293F	11.961	1.0	1.0	1.0	2.1	6.7	23.4	1.5	3.0	1.6	1.2	1.4	1.1
CH0848d0780.15.29D11gp120/293F	11.937	1.1	1.0	1.1	1.5	2.8	2.9	1.5	2.1	1.5	1.2	1.2	1.1
CH848.3.d0611.20.28D11gp120	11.897	1.1	1.0	1.1	1.3	15.9	40.7	1.7	5.0	1.8	1.3	1.2	1.2
CH848.3.d0864.7.39D11gp120	11.794	1.1	1.0	1.1	1.5	3.6	6.7	1.6	2.4	1.7	1.2	1.4	1.2
CH848.3.d0794.5.41D11gp120/293F	11.788	1.0	1.0	1.0	1.4	2.3	2.7	1.4	1.9	1.4	1.1	1.2	1.1
CH848.3.d0611.9.02D11gp120	11.76	1.1	1.0	1.1	1.2	11.3	84.6	1.7	3.8	1.9	1.3	1.2	1.2
CH0848d1432.5.06D11gp120/293F	11.751	1.0	1.1	1.0	2.3	8.4	29.9	1.6	3.4	1.7	1.2	1.4	1.1
CH0848d0780.25.05D11gp120	11.207	1.1	1.2	1.1	3.2	NB	NB	2.8	45.4	3.5	1.8	1.6	1.4
CH0848d0808.15.43D11gp120/293F	11.649	1.1	1.0	1.1	2.1	6.8	8.1	1.7	3.9	1.9	1.3	1.4	1.2
CH848.3.d1621.4.44D11gp120/293F	11.346	1.1	1.1	1.0	2.0	NB	27.4	1.7	28.9	1.7	1.5	1.7	1.3
CH848.3.d0358.80.44D11gp120	11.275	1.2	1.1	1.2	2.5	NB	78.3	2.0	32.8	2.2	1.6	1.5	1.3
CH848.3.d0526.25.21D11gp120	11.116	1.1	1.0	1.1	2.6	NB	NB	2.1	17.4	2.5	1.6	1.6	1.3
CH848.3.d0274.30.09D11gp120/293F	10.95	1.2	1.4	1.2	2.8	NB	121.7	2.2	33.8	2.5	1.7	1.6	1.4
CH848.3.d0700.15.29D11gp120/293F	10.942	1.1	1.0	1.1	3.2	NB	NB	2.9	43.4	3.8	1.8	1.7	1.4
CH848.3.d0358.80.17D11gp120/293F	10.918	1.2	1.1	1.2	3.0	NB	NB	2.4	37.8	2.8	1.7	1.6	1.4
CH848.3.d1120.10.24D11gp120/293i/PEI	10.849	1.1	1.0	1.1	1.8	5.2	10.8	1.7	3.0	1.9	1.3	1.6	1.2
CH848.3.d0893.10.06D11gp120/293F	10.793	1.1	1.0	1.1	1.4	7.0	29.7	1.7	3.5	2.0	1.3	1.6	1.2
CH848.3.d0445.25.26D11gp120/293F	10.782	1.2	1.1	1.2	3.3	NB	136.5	2.7	113.5	3.3	1.8	1.6	1.5
CH0848d0780.15.22D11gp120/293VRC	10.781	1.1	1.0	1.1	2.1	3.8	4.8	2.0	3.1	2.3	1.5	1.5	1.3
CH848.3.d0107.30.27D11gp120/293F	10.704	1.2	1.7	1.2	3.2	NB	65.7	2.2	127.4	2.5	1.6	1.7	1.4
CH848.3.d0700.15.15D11gp120	10.6	1.2	1.4	1.2	3.7	NB	NB	3.5	108.2	4.9	2.0	1.7	1.4
CH848.3.d0836.10.36D11gp120/293F	10.547	1.1	1.2	1.1	1.7	4.8	11.3	1.8	2.9	2.0	1.3	1.8	1.2
CH0848d1120.10.05D11gp120/293F	10.483	1.1	1.0	1.0	1.5	6.5	9.7	1.6	2.9	1.7	1.1	1.4	1.1
CH848.3.d0445.30.42D11gp120	10.474	1.2	1.1	1.2	4.0	NB	NB	3.2	45.0	3.9	1.9	1.8	1.5
CH848.3.d1432.5.18D11gp120/293F	10.33	1.1	1.2	1.0	2.6	NB	69.3	2.1	100.3	2.1	1.7	2.0	1.3
CH848.3.d0135.60.05D11gp120	10.327	1.2	1.2	1.2	3.5	NB	77.1	2.4	NB	2.5	1.8	1.6	1.4
CH0848d0794.3.03D11gp120/293F	10.326	1.0	1.1	1.1	1.1	24.7	109.9	2.1	3.5	3.1	1.4	1.1	1.4
CH848.3.d0526.25.10D11gp120/293F	10.064	1.2	1.2	1.2	4.4	NB	NB	3.8	NB	5.5	2.0	1.8	1.5
CH848.3.d1432.5.27D11gp120/293F	9.881	1.1	1.0	1.1	1.5	6.3	4.2	1.6	2.5	1.8	1.2	0.9	1.3
CH848.3.d0194.25.17D11gp120	9.785	1.2	1.1	1.2	4.7	NB	NB	4.0	NB	5.5	1.9	1.8	1.4
CH848.3.d0135.60.20D11gp120/293F	9.757	1.2	1.3	1.2	3.7	NB	NB	2.8	NB	3.2	1.9	1.7	1.4
CH848.3.d0107.30.31D11gp120/293F	9.647	1.3	2.0	1.3	4.4	NB	NB	3.4	NB	3.9	2.0	1.9	1.5
CH848.3.d0611.20.12D11gp120/293F	9.641	1.2	1.1	1.1	1.6	NB	NB	2.7	15.2	3.7	1.7	1.6	1.4
CH0848.3 TF gp120	9.615	1.1	1.1	1.2	3.4	NB	NB	2.8	NB	2.9	1.8	1.6	1.3
CH848.3.d0078.30.42D11gp120/293F	9.515	1.2	1.2	1.2	3.8	NB	NB	2.8	NB	3.1	1.9	1.7	1.4
CH848.3.d1651.10.04D11gp120/293F	9.341	1.2	1.1	1.1	2.9	NB	NB	3.8	NB	4.5	2.0	3.0	1.5
CH848.3.d0107.30.12D11gp120	9.12	1.3	1.5	1.2	4.4	NB	NB	4.0	NB	4.6	2.1	1.9	1.5
CH848.3.d0445.25.04D11gp120/293F	9.026	1.3	1.1	1.2	4.9	NB	NB	4.7	NB	8.3	2.2	1.8	1.6
CH848.3.d1432.5.56D11gp120/293F	8.83	1.3	1.5	1.1	3.2	NB	NB	2.8	NB	2.8	1.9	2.6	1.4
CH848.3.d1621.4.15D11gp120/293F	8.805	1.3	1.2	1.2	5.9	NB	NB	7.8	NB	11.2	2.5	2.1	1.6
CH848.3.d0078.30.02D11gp120	8.763	1.3	0.9	1.2	4.1	NB	NB	3.8	NB	4.5	2.1	1.9	1.4
CH848.3.d1677.521.D11gp120/293F	8.713	1.2	1.2	1.1	2.5	NB	NB	3.4	NB	3.3	1.9	2.8	1.4
CH848.3.d1120.10.21D11gp120/293F/PEI	8.698	1.2	1.0	1.2	2.6	NB	NB	3.2	22.9	3.2	1.9	2.8	1.6
CH848.3.d0274.30.07D11gp120/293F	8.693	1.2	1.1	1.2	5.0	NB	NB	4.7	NB	5.1	2.3	2.1	1.7
CH0848d0949.10.18D11gp120/293F	8.648	1.1	1.1	1.1	1.6	9.1	9.7	1.9	2.8	2.5	1.4	1.2	1.4
CH848.3.d0526.25.32D11gp120	8.101	1.3	1.2	1.3	7.5	NB	NB	10.3	NB	19.2	2.8	2.6	2.0
CH0848d0526.25.26D11gp120/293F	8.083	1.3	1.0	1.2	6.1	NB	NB	6.9	NB	10.8	2.6	2.3	1.8
CH848.3.d1651.7.34D11gp120/293F	7.959	1.2	1.2	1.1	3.1	NB	NB	4.2	NB	4.9	2.1	3.9	1.5
CH848.3.d0135.60.32D11gp120/293F	7.94	1.3	1.3	1.3	6.9	NB	NB	7.9	NB	10.1	2.7	2.5	1.7
CH848.3.d0358.80.03D11gp120/293F	7.573	1.3	1.2	1.3	7.9	NB	NB	6.6	NB	11.8	2.6	1.9	1.7
CH0848d0780.15.22D11gp120/293F	7.567	1.2	1.0	1.2	2.8	5.9	8.8	2.7	4.4	3.2	1.8	2.0	1.6
CH848.3.d0526.25.39D11gp120	7.567	1.4	1.5	1.3	7.8	NB	NB	10.1	NB	15.7	2.9	2.3	1.9
CH848.3.d1621.4.31D11gp120/293F	7.39	1.4	1.2	1.1	3.8	NB	NB	7.1	NB	7.9	2.4	4.4	1.6
CH848.3.d0700.27.06D11gp120/293F	7.219	1.2	1.3	1.1	0.7	NB	NB	11.2	NB	26.1	3.1	1.3	2.6
CH848.3.d0135.60.34D11gp120/293F	6.983	1.5	1.4	1.3	6.8	NB	NB	8.6	NB	10.9	2.9	2.6	1.9
CH0848d0864.3.03D11gp120/293F	6.867	1.1	1.2	1.2	1.1	NB	NB	3.9	9.0	8.5	2.0	1.2	1.9
CH848.3.d0526.25.11D11gp120/293F	6.793	1.3	0.9	1.3	11.9	NB	NB	10.0	NB	15.7	2.7	4.7	2.0
CH848.3.d1621.4.12D11gp120/293F	6.676	1.8	1.5	1.3	5.4	NB	NB	48.4	NB	63.0	3.7	2.9	3.1
CH848.3.d1720.5D11gp120/293F	6.366	1.4	0.9	1.5	24.6	NB	NB	11.9	NB	14.7	3.2	5.2	2.3
CH848.3.d0274.30.14D11gp120/293F	6.191	1.5	1.1	1.5	16.6	NB	NB	23.5	NB	63.2	3.8	3.5	2.9
CH848.3.d0274.30.02D11gp120/293F	4.89	1.6	1.1	1.5	16.9	NB	NB	20.4	NB	26.3	4.2	3.6	3.0
CH848.3.d0445.25.18D11gp120	4.764	1.5	1.4	1.5	20.3	NB	NB	36.1	NB	NB	4.6	3.6	2.9
CH848.3.d0135.60.19D11gp120/293F	4.562	1.7	1.1	1.4	11.9	NB	NB	31.9	NB	40.4	3.7	3.9	2.8
CH0848d0700.15.05D11gp120/293F	4.512	1.4	1.3	1.4	12.6	NB	NB	NB	NB	NB	5.7	5.1	3.1
CH0848d0949.10.10D11gp120/293F	3.471	1.2	1.1	1.3	1.1	NB	NB	6.6	11.1	46.3	2.9	1.8	2.4
CH848.3.d0445.30.41D11gp120	2.985	1.7	1.1	1.5	26.9	NB	NB	NB	NB	NB	4.9	5.2	3.6
CH848.3.d0611.20.14D11gp120	2.949	1.7	1.1	1.3	2.1	NB	NB	18.4	NB	NB	4.0	2.7	2.4
CH848.3.d1120.10.13D11gp120/293F	2.528	1.1	1.1	1.1	1.4	NB	NB	6.5	18.5	19.0	2.4	1.5	2.1
CH848.3.d0194.25.24D11gp120/293F	2.23	2.2	1.1	1.9	NB	NB	NB	NB	NB	NB	8.7	5.2	5.6
CH848.3.d0194.25.21D11gp120	2.192	1.7	2.5	1.6	NB	NB	NB	NB	NB	NB	8.5	9.7	4.6
CH0848d0893.10.05D11gp120/293F	2.174	1.1	1.3	1.3	1.0	NB	NB	7.3	11.4	NB	3.0	1.8	2.4
CH848.3.d0135.60.14D11gp120/293F	1.464	2.1	1.0	2.1	NB	NB	NB	NB	NB	NB	20.1	NB	8.3
CH848.3.d0194.25.48D11gp120/293F	0.584	6.3	1.1	3.2	NB	NB	NB	NB	NB	NB	NB	5.4	NB
CH848.3.d1305.10.35D11gp120/293F	0.092	NB	NB	0.4	0.1	NB	NB	NB	NB	NB	NB	NB	NB
CH0848d1432.5.35D11gp120/293F	0	NB	NB	NB	NB	NB	NB	NB	NB	NB	NB	NB	NB
CH848.3.d1305.10.13D11gp120/293F	0	NB	NB	NB	NB	NB	NB	NB	NB	NB	NB	NB	NB
CH848.3.d1305.10.21D11gp120/293F	0	NB	NB	NB	NB	NB	NB	NB	NB	NB	NB	NB	NB
CH848.3.d1305.10.30D11gp120/293F	0	NB	NB	NB	NB	NB	NB	NB	NB	NB	NB	NB	NB
CH848.3.d1432.5.50D11gp120	0	NB	NB	NB	NB	NB	NB	NB	NB	NB	NB	NB	NB
CH848.3.d1621.4.25D11gp120	0	NB	NB	NB	NB	NB	NB	NB	NB	NB	NB	NB	NB
CH848.3.d1621.4.46D11gp120	0	NB	NB	NB	NB	NB	NB	NB	NB	NB	NB	NB	NB
CH848.3.d1651.7.50D11gp120/293F	0	NB	NB	NB		NB	NB	NB	NB	NB	NB	NB	NB
CH848.d1651.10.07D11gp120/293F	0	NB	NB	NB	NB	NB	NB	NB	NB	NB	NB	NB	NB

	<1 fold
	1-2 fold
	2-5 fold
	5-10 fold
	10-25 fold
	25-50 fold
	>50 fold
NB	no binding

Supplementary Figure 3. Interactions of candidate gp120 immunogens with DH270min1 antibody variants. ELISA binding of mutated DH270min1 antibodies with each acquired mutation changed to the corresponding UCA residue to a panel of gp120 immunogen candidates. Values represent fold decrease in binding of a given gp120 to a respective DH270min1 mutated antibody relative to its binding to the unmutated DH270min1 mAb. Highlighted molecules at the top of the table were considered for further analysis. Binding values (logAUC) to DH270min1 are shown as reference. NB=not binding.

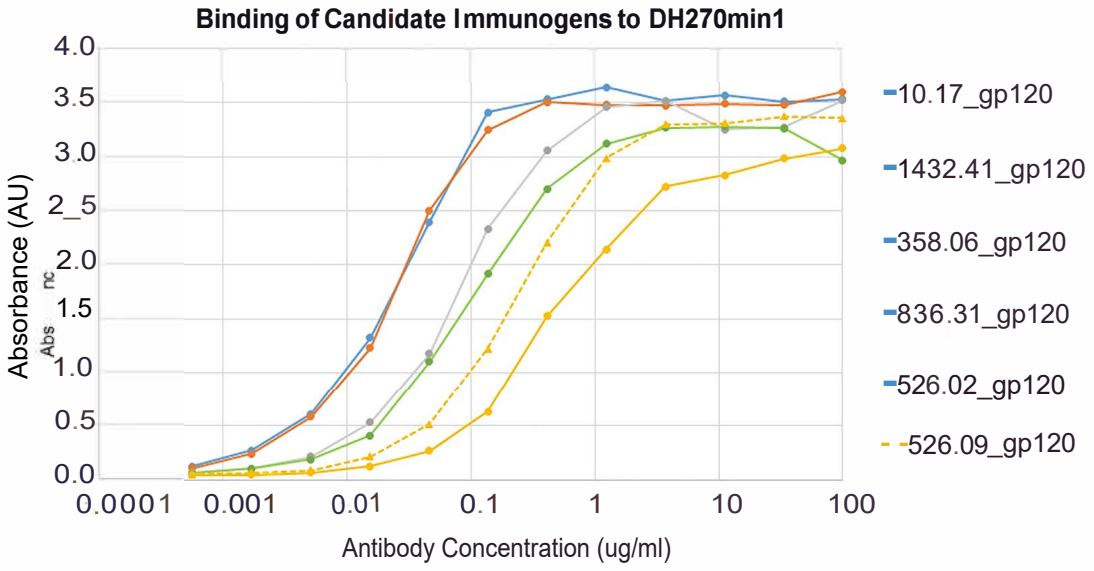

Supplementary Figure 4. ELISA binding of candidate immunogen gp120s to DH270min1. The binding of DH270min1 was measured to immunogen candidates by ELISA suggests an affinity gradient exists amongst the immunogen candidates. This correlates with previous data that these viruses are progressively more difficult to neutralize described in Supplementary Figure 6 and supports the use of these immunogens in sequential prime/boost strategy.

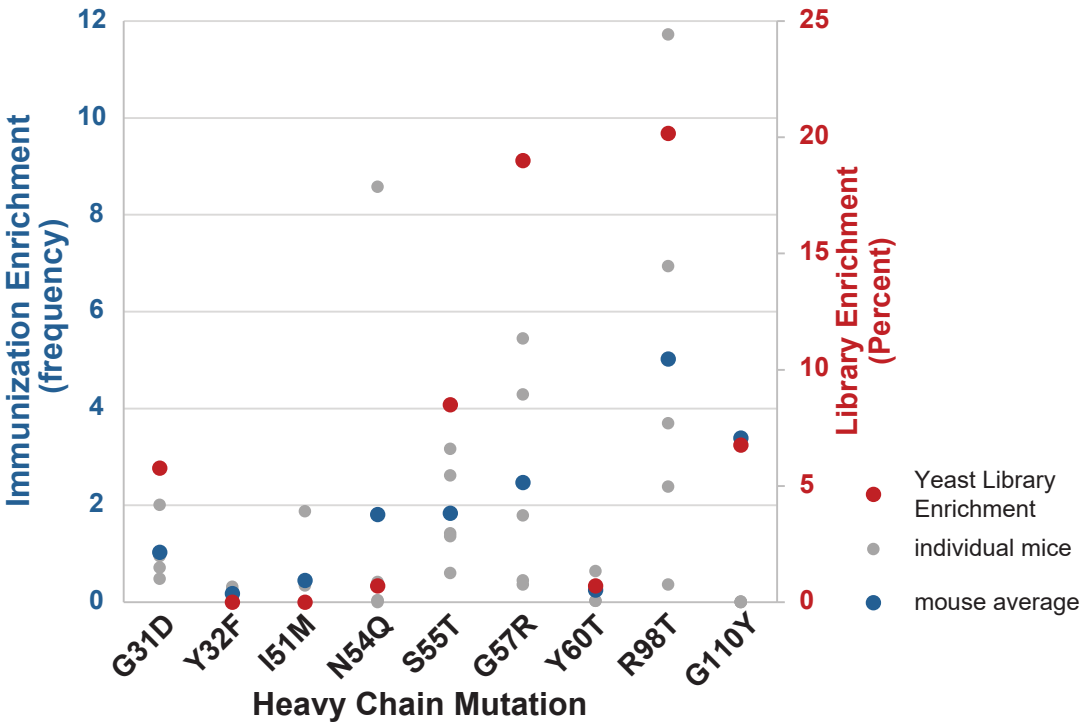

Supplementary Figure 5. Correlation between the amino acids selected from the scFv library by 10.17DT and the acquired mutations in the antibodies elicited by immunizations with 10.17DT. The same values as in Figure 4D, individually plotted. Negative library enrichment values are plotted as 0. The enrichment of mutations by 10.17DT vaccination in mice and the enrichment of yeast library clones selected by 10.17DT (y-axis) plotted against heavy chain mutation. Library enrichment values were calculated as described in Figure 4C. For immunization enrichment, both the data from individual animals (gray, dashed) and the calculated average (blue) is displayed.

Virus	V1 loop length	DH270.UCA	DH270.IA4	DH270.IA3	DH270.IA2	DH270.IA1	DH270.5	DH270.min11
CH848.0949.10.17	17	>50	0.64	0.2	0.14	<0.02	0.05	0.42
CH848.0358.80.06	24	>50	>50	>50	>50	0.02	<0.02	0.026
CH848.1432.5.41	30	>50	>50	>50	>50	0.33	0.21	<0.023

IC50 ug/ml
<0.1
0.1 to <1
1 to <10
10 to 50
>50

Supplementary Figure 6. DH270min11 neutralization of pseudoviruses that containin the Envs used for the analysis of scFv libraries. Values indicate IC_{50} neutralization values of DH270 lineage precursor antibodies and DH270min11 mAb against pseudoviruses containing Envs that were used to develop the immunogens described in Figures 3, 4 and 5. DH270.IA4, DH270.IA3, DH270.IA2, DH270IA1 and DH270.5 are DH270 lineage members that are progressively closer in sequence to DH270.6 as previously described (Bonsignori et al., 2017). Neutralization data for these mAbs comes from (Bonsignori et al., 2017).

$M51_{HC}$			$T55_{HC}$			$R57_{HC}$			$A97_{LC}$		
Probability	**10.17DT**	**1432**	**Probability**	**10.17DT**	**1432**	**Probability**	**10.17DT**	**1432**	**Probability**	**10.17DT**	**1432**
M=0.01914	**8.20%**	**4.10%**	**T=0.04783**	**46.30%**	**12.80%**	**R=0.01415**	**20.30%**	**19.50%**	**A=0.00431**	**35.90%**	**14.70%**
V= 0.04787	19.50%	18.70%	S=0.71751	13.80%	10.10%	G=0.78281	3.70%	10.10%	S=0.41163	6.20%	8.60%
L=0.03062	20.30%	13.30%	R=0.07251	14.20%	18.10%	A=0.04853	20.50%	12.70%	R=0.26982	2.70%	12.40%
T=0.02859	2.10%	2.40%	G=0.04371	3.20%	12%	V=0.02853	3.90%	5.10%	G=0.06867	47.60%	23.60%
S=0.01854	2.90%	4.90%	A=0.00209	4.40%	8.10%	E=0.00939	3.90%	3.60%	T=0.04228	0.60%	4.20%
F=0.01067	1.20%	0.70%	V=0.00102	2.10%	6.20%	S=0.00659	9.30%	8.30%	D=0.01041	1%	3.60%
R=0.00581	2.60%	7.60%	L=0.00077	8%	8.80%	L=0.00043	4.40%	5.50%	L=0.00376	0.40%	2.90%
A=0.00166	2.30%	5.20%	W=0.0006	1.40%	5.30%	P=0.00041	0.20%	3.90%	W=0.00199	1.30%	3.60%
G=0.00076	3.00%	9.50%	M=0.00042	0.80%	3.10%	W=0.00013	1.80%	2.90%	P=0.00172	0.40%	4.30%
E=0.0001	2.50%	4.50%	Q=0.00017	0.80%	2.40%	T=0.00125	14.30%	10.80%	E=0.00113	1.60%	6.10%
C=0.00019	5.80%	3.00%				Q=0.00011	4.60%	4%			
W=0.00001	3.80%	3.80%				H=0.00104	2.80%	2.40%			
						M=0.00003	2.40%	2.40%			

DH270.6
more probable than DH270.6
similar probability to DH270.6

Supplementary Figure 7. The ARMADiLLO predicted probability of DH270min11 alternate amino acids identified by screening to occur *in vivo*. ARMADiLLO calculated probabilities of alternate amino acids identified at the V3 loop contacting sites of DH270min11 by the library screening approach described in Figure 5. Residues present in the mature DH270.6 and their expected *in vivo* probability are shown in blue. Frequencies of each amino acid present in the clones isolated after sorts with 10.17DT and 1432.41 SOSIPs are reported as percent of total.

590 # References

591 Abbott, R.K., Lee, J.H., Menis, S., Skog, P., Rossi, M., Ota, T., Kulp, D.W., Bhullar, D., Kalyuzhniy, O.,
592 Havenar-Daughton, C.*, et al.* (2018). Precursor Frequency and Affinity Determine B Cell Competitive
593 Fitness in Germinal Centers, Tested with Germline-Targeting HIV Vaccine Immunogens. Immunity *48*,
594 133-146.e136.
595 Alam, S.M., Aussedat, B., Vohra, Y., Meyerhoff, R.R., Cale, E.M., Walkowicz, W.E., Radakovich, N.A.,
596 Anasti, K., Armand, L., Parks, R.*, et al.* (2017). Mimicry of an HIV broadly neutralizing antibody epitope
597 with a synthetic glycopeptide. Science Translational Medicine *9*, eaai7521.
598 Alam, S.M., Liao, H.-X., Tomaras, G.D., Bonsignori, M., Tsao, C.-Y., Hwang, K.-K., Chen, H., Lloyd, K.E.,
599 Bowman, C., Sutherland, L.*, et al.* (2013). Antigenicity and Immunogenicity of RV144 Vaccine AIDSVAX
600 Clade E Envelope Immunogen Is Enhanced by a gp120 N-Terminal Deletion. Journal of Virology *87*, 1554-
601 1568.
602 Barnes, C.O., Gristick, H.B., Freund, N.T., Escolano, A., Lyubimov, A.Y., Hartweger, H., West, A.P., Cohen,
603 A.E., Nussenzweig, M.C., and Bjorkman, P.J. (2018). Structural characterization of a highly-potent V3-
604 glycan broadly neutralizing antibody bound to natively-glycosylated HIV-1 envelope. Nature
605 Communications *9*, 1251.
606 Benatuil, L., Perez, J.M., Belk, J., and Hsieh, C.M. (2010). An improved yeast transformation method for
607 the generation of very large human antibody libraries. Protein Eng Des Sel *23*, 155-159.
608 Bender, B.J., Cisneros, A., Duran, A.M., Finn, J.A., Fu, D., Lokits, A.D., Mueller, B.K., Sangha, A.K., Sauer,
609 M.F., Sevy, A.M.*, et al.* (2016). Protocols for Molecular Modeling with Rosetta3 and RosettaScripts.
610 Biochemistry *55*, 4748-4763.
611 Bonsignori, M., Kreider, E.F., Fera, D., Meyerhoff, R.R., Bradley, T., Wiehe, K., Alam, S.M., Aussedat, B.,
612 Walkowicz, W.E., Hwang, K.K.*, et al.* (2017a). Staged induction of HIV-1 glycan-dependent broadly
613 neutralizing antibodies. Sci Transl Med *9*.
614 Bonsignori, M., Liao, H.X., Gao, F., Williams, W.B., Alam, S.M., Montefiori, D.C., and Haynes, B.F. (2017b).
615 Antibody-virus co-evolution in HIV infection: paths for HIV vaccine development. Immunol Rev *275*, 145-
616 160.
617 Bonsignori, M., Scott, E., Wiehe, K., Easterhoff, D., Alam, S.M., Hwang, K.K., Cooper, M., Xia, S.M., Zhang,
618 R., Montefiori, D.C.*, et al.* (2018). Inference of the HIV-1 VRC01 Antibody Lineage Unmutated Common
619 Ancestor Reveals Alternative Pathways to Overcome a Key Glycan Barrier. Immunity *49*, 1162-
620 1174.e1168.
621 Bonsignori, M., Zhou, T., Sheng, Z., Chen, L., Gao, F., Joyce, M.G., Ozorowski, G., Chuang, G.-Y., Schramm,
622 C.A., Wiehe, K.*, et al.* (2016). Maturation Pathway from Germline to Broad HIV-1 Neutralizer of a CD4-
623 Mimic Antibody. Cell *165*, 449-463.
624 Briney, B., Sok, D., Jardine, J.G., Kulp, D.W., Skog, P., Menis, S., Jacak, R., Kalyuzhniy, O., de Val, N.,
625 Sesterhenn, F.*, et al.* (2016). Tailored Immunogens Direct Affinity Maturation toward HIV Neutralizing
626 Antibodies. Cell *166*, 1459-1470.e1411.
627 Cao, L., Diedrich, J.K., Kulp, D.W., Pauthner, M., He, L., Park, S.-K.R., Sok, D., Su, C.Y., Delahunty, C.M.,
628 Menis, S.*, et al.* (2017). Global site-specific N-glycosylation analysis of HIV envelope glycoprotein. Nature
629 Communications *8*, 14954.
630 Chao, G., Lau, W.L., Hackel, B.J., Sazinsky, S.L., Lippow, S.M., and Wittrup, K.D. (2006). Isolating and
631 engineering human antibodies using yeast surface display. Nature Protocols *1*, 755-768.
632 Das, R., and Baker, D. (2008). Macromolecular Modeling with Rosetta. Annual Review of Biochemistry
633 *77*, 363-382.
634 Doria-Rose, N.A., Klein, R.M., Daniels, M.G., Dell, S., Nason, M., Lapedes, A., Bhattacharya, T., Migueles,
635 S.A., Wyatt, R.T., Korber, B.T.*, et al.* (2010). Breadth of Human Immunodeficiency Virus-Specific

636 Neutralizing Activity in Sera: Clustering Analysis and Association with Clinical Variables. Journal of
637 Virology *84*, 1631.
638 Doria-Rose, N.A., and Landais, E. (2019). Coevolution of HIV-1 and broadly neutralizing antibodies. Curr
639 Opin HIV AIDS *14*, 286-293.
640 Dosenovic, P., von Boehmer, L., Escolano, A., Jardine, J., Freund, N.T., Gitlin, A.D., McGuire, A.T., Kulp,
641 D.W., Oliveira, T., Scharf, L.*, et al.* (2015a). Immunization for HIV-1 Broadly Neutralizing Antibodies in
642 Human Ig Knockin Mice. Cell *161*, 1505-1515.
643 Dosenovic, P., von Boehmer, L., Escolano, A., Jardine, J., Freund, Natalia T., Gitlin, Alexander D.,
644 McGuire, Andrew T., Kulp, Daniel W., Oliveira, T., Scharf, L.*, et al.* (2015b). Immunization for HIV-1
645 Broadly Neutralizing Antibodies in Human Ig Knockin Mice. Cell *161*, 1505-1515.
646 Escolano, A., Steichen, J.M., Dosenovic, P., Kulp, D.W., Golijanin, J., Sok, D., Freund, N.T., Gitlin, A.D.,
647 Oliveira, T., Araki, T.*, et al.* (2016). Sequential Immunization Elicits Broadly Neutralizing Anti-HIV-1
648 Antibodies in Ig Knockin Mice. Cell *166*, 1445-1458.e1412.
649 Fera, D., Lee, M.S., Wiehe, K., Meyerhoff, R.R., Piai, A., Bonsignori, M., Aussedat, B., Walkowicz, W.E.,
650 Ton, T., Zhou, J.O.*, et al.* (2018). HIV envelope V3 region mimic embodies key features of a broadly
651 neutralizing antibody lineage epitope. Nature Communications *9*, 1111.
652 Freund, N.T., Wang, H., Scharf, L., Nogueira, L., Horwitz, J.A., Bar-On, Y., Golijanin, J., Sievers, S.A., Sok,
653 D., Cai, H.*, et al.* (2017). Coexistence of potent HIV-1 broadly neutralizing antibodies and antibody-
654 sensitive viruses in a viremic controller. Sci Transl Med *9*.
655 Gao, F., Bonsignori, M., Liao, H.X., Kumar, A., Xia, S.M., Lu, X., Cai, F., Hwang, K.K., Song, H., Zhou, T.*, et*
656 *al.* (2014). Cooperation of B cell lineages in induction of HIV-1-broadly neutralizing antibodies. Cell *158*,
657 481-491.
658 Georgiev, I.S., Rudicell, R.S., Saunders, K.O., Shi, W., Kirys, T., McKee, K., O'Dell, S., Chuang, G.-Y., Yang,
659 Z.-Y., Ofek, G.*, et al.* (2014). Antibodies VRC01 and 10E8 Neutralize HIV-1 with High Breadth and Potency
660 Even with Ig-Framework Regions Substantially Reverted to Germline. The Journal of Immunology *192*,
661 1100.
662 Gray, E.S., Taylor, N., Wycuff, D., Moore, P.L., Tomaras, G.D., Wibmer, C.K., Puren, A., DeCamp, A.,
663 Gilbert, P.B., Wood, B.*, et al.* (2009). Antibody Specificities Associated with Neutralization Breadth in
664 Plasma from Human Immunodeficiency Virus Type 1 Subtype C-Infected Blood Donors. Journal of
665 Virology *83*, 8925.
666 Havenar-Daughton, C., Sarkar, A., Kulp, D.W., Toy, L., Hu, X., Deresa, I., Kalyuzhniy, O., Kaushik, K.,
667 Upadhyay, A.A., Menis, S.*, et al.* (2018). The human naive B cell repertoire contains distinct subclasses
668 for a germline-targeting HIV-1 vaccine immunogen. Science translational medicine *10*, eaat0381.
669 Haynes, B.F., Burton, D.R., and Mascola, J.R. (2019). Multiple roles for HIV broadly neutralizing
670 antibodies. Science Translational Medicine *11*, eaaz2686.
671 Haynes, B.F., Kelsoe, G., Harrison, S.C., and Kepler, T.B. (2012). B-cell-lineage immunogen design in
672 vaccine development with HIV-1 as a case study. Nat Biotechnol *30*, 423-433.
673 Haynes, B.F., Shaw, G.M., Korber, B., Kelsoe, G., Sodroski, J., Hahn, B.H., Borrow, P., and McMichael, A.J.
674 (2016). HIV-Host Interactions: Implications for Vaccine Design. Cell Host Microbe *19*, 292-303.
675 Hraber, P., Seaman, M.S., Bailer, R.T., Mascola, J.R., Montefiori, D.C., and Korber, B.T. (2014). Prevalence
676 of broadly neutralizing antibody responses during chronic HIV-1 infection. Aids *28*, 163-169.
677 Hwang, J.K., Wang, C., Du, Z., Meyers, R.M., Kepler, T.B., Neuberg, D., Kwong, P.D., Mascola, J.R., Joyce,
678 M.G., Bonsignori, M.*, et al.* (2017). Sequence intrinsic somatic mutation mechanisms contribute to
679 affinity maturation of VRC01-class HIV-1 broadly neutralizing antibodies. Proc Natl Acad Sci U S A *114*,
680 8614-8619.
681 Jardine, J.G., Sok, D., Julien, J.P., Briney, B., Sarkar, A., Liang, C.H., Scherer, E.A., Henry Dunand, C.J.,
682 Adachi, Y., Diwanji, D.*, et al.* (2016). Minimally Mutated HIV-1 Broadly Neutralizing Antibodies to Guide
683 Reductionist Vaccine Design. PLoS Pathog *12*, e1005815.

684 Julien, J.-P., Sok, D., Khayat, R., Lee, J.H., Doores, K.J., Walker, L.M., Ramos, A., Diwanji, D.C., Pejchal, R.,
685 Cupo, A.*, et al.* (2013). Broadly neutralizing antibody PGT121 allosterically modulates CD4 binding via
686 recognition of the HIV-1 gp120 V3 base and multiple surrounding glycans. PLoS pathogens *9*, e1003342-
687 e1003342.
688 Kepler, T.B., Liao, H.-X., Alam, S.M., Bhaskarabhatla, R., Zhang, R., Yandava, C., Stewart, S., Anasti, K.,
689 Kelsoe, G., Parks, R.*, et al.* (2014). Immunoglobulin gene insertions and deletions in the affinity
690 maturation of HIV-1 broadly reactive neutralizing antibodies. Cell host & microbe *16*, 304-313.
691 Klein, F., Diskin, R., Scheid, Johannes F., Gaebler, C., Mouquet, H., Georgiev, I.S., Pancera, M., Zhou, T.,
692 Incesu, R.-B., Fu, Brooks Z.*, et al.* (2013). Somatic Mutations of the Immunoglobulin Framework Are
693 Generally Required for Broad and Potent HIV-1 Neutralization. Cell *153*, 126-138.
694 Kwong, P.D., and Mascola, J.R. (2018). HIV-1 Vaccines Based on Antibody Identification, B Cell Ontogeny,
695 and Epitope Structure. Immunity *48*, 855-871.
696 LaBranche, C.C., Henderson, R., Hsu, A., Behrens, S., Chen, X., Zhou, T., Wiehe, K., Saunders, K.O., Alam,
697 S.M., Bonsignori, M.*, et al.* (2019). Neutralization-guided design of HIV-1 envelope trimers with high
698 affinity for the unmutated common ancestor of CH235 lineage CD4bs broadly neutralizing antibodies.
699 PLOS Pathogens *15*, e1008026.
700 Landais, E., and Moore, P.L. (2018). Development of broadly neutralizing antibodies in HIV-1 infected
701 elite neutralizers. Retrovirology *15*, 61.
702 Lauck, F., Smith, C.A., Friedland, G.F., Humphris, E.L., and Kortemme, T. (2010). RosettaBackrub—a web
703 server for flexible backbone protein structure modeling and design. Nucleic Acids Research *38*, W569-
704 W575.
705 Leaver-Fay, A., Tyka, M., Lewis, S.M., Lange, O.F., Thompson, J., Jacak, R., Kaufman, K., Renfrew, P.D.,
706 Smith, C.A., Sheffler, W.*, et al.* (2011). ROSETTA3: an object-oriented software suite for the simulation
707 and design of macromolecules. Methods Enzymol *487*, 545-574.
708 Lee, J.H., Nakao, C., Moyer, T.J., Irvine, D.J., Schief, W.R., and Crotty, S. (2020). Exploration of roles of
709 CD4 T cell help in recruitment of rare B cells to germinal centers. The Journal of Immunology *204*,
710 167.165.
711 Liao, H.-X., Bonsignori, M., Alam, S.M., McLellan, Jason S., Tomaras, Georgia D., Moody, M.A., Kozink,
712 Daniel M., Hwang, K.-K., Chen, X., Tsao, C.-Y.*, et al.* (2013a). Vaccine Induction of Antibodies against a
713 Structurally Heterogeneous Site of Immune Pressure within HIV-1 Envelope Protein Variable Regions 1
714 and 2. Immunity *38*, 176-186.
715 Liao, H.-X., Sutherland, L.L., Xia, S.-M., Brock, M.E., Scearce, R.M., Vanleeuwen, S., Alam, S.M.,
716 McAdams, M., Weaver, E.A., Camacho, Z.T.*, et al.* (2006). A group M consensus envelope glycoprotein
717 induces antibodies that neutralize subsets of subtype B and C HIV-1 primary viruses. Virology *353*, 268-
718 282.
719 Liao, H.X., Lynch, R., Zhou, T., Gao, F., Alam, S.M., Boyd, S.D., Fire, A.Z., Roskin, K.M., Schramm, C.A.,
720 Zhang, Z.*, et al.* (2013b). Co-evolution of a broadly neutralizing HIV-1 antibody and founder virus. Nature
721 *496*, 469-476.
722 Mesin, L., Schiepers, A., Ersching, J., Barbulescu, A., Cavazzoni, C.B., Angelini, A., Okada, T., Kurosaki, T.,
723 and Victora, G.D. (2020). Restricted Clonality and Limited Germinal Center Reentry Characterize Memory
724 B Cell Reactivation by Boosting. Cell *180*, 92-106.e111.
725 Mouquet, H., Scharf, L., Euler, Z., Liu, Y., Eden, C., Scheid, J.F., Halper-Stromberg, A., Gnanapragasam,
726 P.N.P., Spencer, D.I.R., Seaman, M.S.*, et al.* (2012). Complex-type N-glycan recognition by potent broadly
727 neutralizing HIV antibodies. Proceedings of the National Academy of Sciences of the United States of
728 America *109*, E3268-E3277.
729 Sanders, R.W., van Gils, M.J., Derking, R., Sok, D., Ketas, T.J., Burger, J.A., Ozorowski, G., Cupo, A.,
730 Simonich, C., Goo, L.*, et al.* (2015). HIV-1 neutralizing antibodies induced by native-like envelope trimers.
731 Science *349*, aac4223.

732 Saunders, K.O., Wiehe, K., Tian, M., Acharya, P., Bradley, T., Alam, S.M., Go, E.P., Scearce, R., Sutherland,
733 L., Henderson, R.*, et al.* (2019). Targeted selection of HIV-specific antibody mutations by engineering B
734 cell maturation. Science *366*.
735 Shen, C.H., DeKosky, B.J., Guo, Y., Xu, K., Gu, Y., Kilam, D., Ko, S.H., Kong, R., Liu, K., Louder, M.K.*, et al.*
736 (2020). VRC34-Antibody Lineage Development Reveals How a Required Rare Mutation Shapes the
737 Maturation of a Broad HIV-Neutralizing Lineage. Cell Host Microbe *27*, 531-543 e536.
738 Simonich, C.A., Williams, K.L., Verkerke, H.P., Williams, J.A., Nduati, R., Lee, K.K., and Overbaugh, J.
739 (2016). HIV-1 Neutralizing Antibodies with Limited Hypermutation from an Infant. Cell *166*, 77-87.
740 Sok, D., Laserson, U., Laserson, J., Liu, Y., Vigneault, F., Julien, J.P., Briney, B., Ramos, A., Saye, K.F., Le, K.*,*
741 *et al.* (2013). The effects of somatic hypermutation on neutralization and binding in the PGT121 family
742 of broadly neutralizing HIV antibodies. PLoS Pathog *9*, e1003754.
743 Steichen, J.M., Kulp, D.W., Tokatlian, T., Escolano, A., Dosenovic, P., Stanfield, R.L., McCoy, L.E.,
744 Ozorowski, G., Hu, X., Kalyuzhniy, O.*, et al.* (2016). HIV Vaccine Design to Target Germline Precursors of
745 Glycan-Dependent Broadly Neutralizing Antibodies. Immunity *45*, 483-496.
746 Steichen, J.M., Lin, Y.C., Havenar-Daughton, C., Pecetta, S., Ozorowski, G., Willis, J.R., Toy, L., Sok, D.,
747 Liguori, A., Kratochvil, S.*, et al.* (2019). A generalized HIV vaccine design strategy for priming of broadly
748 neutralizing antibody responses. Science *366*.
749 Struwe, W.B., Chertova, E., Allen, J.D., Seabright, G.E., Watanabe, Y., Harvey, D.J., Medina-Ramirez, M.,
750 Roser, J.D., Smith, R., Westcott, D.*, et al.* (2018). Site-Specific Glycosylation of Virion-Derived HIV-1 Env Is
751 Mimicked by a Soluble Trimeric Immunogen. Cell Rep *24*, 1958-1966.e1955.
752 Tian, M., Cheng, C., Chen, X., Duan, H., Cheng, H.-L., Dao, M., Sheng, Z., Kimble, M., Wang, L., Lin, S.*, et*
753 *al.* (2016). Induction of HIV Neutralizing Antibody Lineages in Mice with Diverse Precursor Repertoires.
754 Cell *166*, 1471-1484.e1418.
755 Walker, L.M., Huber, M., Doores, K.J., Falkowska, E., Pejchal, R., Julien, J.P., Wang, S.K., Ramos, A., Chan-
756 Hui, P.Y., Moyle, M.*, et al.* (2011). Broad neutralization coverage of HIV by multiple highly potent
757 antibodies. Nature *477*, 466-470.
758 Wiehe, K., Bradley, T., Meyerhoff, R.R., Hart, C., Williams, W.B., Easterhoff, D., Faison, W.J., Kepler, T.B.,
759 Saunders, K.O., Alam, S.M.*, et al.* (2018). Functional Relevance of Improbable Antibody Mutations for
760 HIV Broadly Neutralizing Antibody Development. Cell Host Microbe *23*, 759-765 e756.
761 Wu, X., Yang, Z.Y., Li, Y., Hogerkorp, C.M., Schief, W.R., Seaman, M.S., Zhou, T., Schmidt, S.D., Wu, L., Xu,
762 L.*, et al.* (2010). Rational design of envelope identifies broadly neutralizing human monoclonal
763 antibodies to HIV-1. Science *329*, 856-861.
764 Wu, X., Zhang, Z., Schramm, C.A., Joyce, M.G., Kwon, Y.D., Zhou, T., Sheng, Z., Zhang, B., O'Dell, S.,
765 McKee, K.*, et al.* (2015). Maturation and Diversity of the VRC01-Antibody Lineage over 15 Years of
766 Chronic HIV-1 Infection. Cell *161*, 470-485.
767 Yaari, G., Vander Heiden, J.A., Uduman, M., Gadala-Maria, D., Gupta, N., Stern, J.N.H., O'Connor, K.C.,
768 Hafler, D.A., Laserson, U., Vigneault, F.*, et al.* (2013). Models of somatic hypermutation targeting and
769 substitution based on synonymous mutations from high-throughput immunoglobulin sequencing data.
770 Front Immunol *4*, 358-358.

771